Design and preliminary operation of a hybrid syngas/solar PV/battery power system for off-grid applications: A case study in Thailand

Kohsri, Sompol; Meechai, Apichart; Prapainainar, Chaiwat; Narataraksa, Phavanee; Hunpinyo, Piyapong; Sin, Gürkan

Published in:
Chemical Engineering Research and Design

Link to article, DOI:
10.1016/j.cherd.2018.01.003

Publication date:
2018

Document Version
Peer reviewed version

Accepted Manuscript

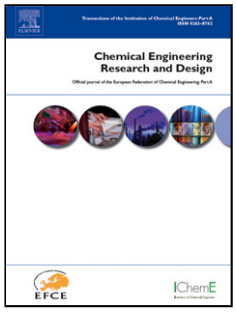

Title: Design and preliminary operation of a hybrid syngas/solar PV/battery power system for off-grid applications: A case study in Thailand

Author: Sompol Kohsri Apichart Meechai Chaiwat Prapainainar Phavanee Narataraksa Piyapong Hunpinyo Gürkan Sin

PII: S0263-8762(18)30005-4
DOI: https://doi.org/doi:10.1016/j.cherd.2018.01.003
Reference: CHERD 2977

To appear in:

Received date: 1-8-2017
Revised date: 20-12-2017
Accepted date: 3-1-2018

Please cite this article as: Kohsri, S., Meechai, A., Prapainainar, C., Narataraksa, P., Hunpinyo, P., Sin, G.,Design and preliminary operation of a hybrid syngas/solar PV/battery power system for off-grid applications: A case study in Thailand, *Chemical Engineering Research and Design* (2018), https://doi.org/10.1016/j.cherd.2018.01.003

Manuscript submission for consideration for possible publication in Chemical Engineering Research and Design (SI: Energy System Engineering)

Design and preliminary operation of a hybrid syngas/solar PV /battery power system for off-grid applications: A case study in Thailand

Sompol Kohsri [a], Apichart Meechai [b], Chaiwat Prapainainar [b,d], Phavanee Narataraksa [b,d], Piyapong Hunpinyo [c,d]*, Gürkan Sin [e]

[a] Division of Instrumentation and Automation Engineering Technology (IAet), 7th floor, EAT Building, Faculty of Engineering and Technology, King Mongkut's University of Technology North Bangkok (Rayong Campus), Thailand.

[b] Department of Chemical Engineering (Ch.E), Faculty of Engineering, King Mongkut's University of Technology North Bangkok, 8th to 15th floors, Buildings 88, 1518 Pracharat 1 Road, Wongsawang, Bangsue, Bangkok 10800, Thailand.

[c] Division of Chemical Process Engineering Technology (CPet), 1st and 3rd floor, EAT Building, Faculty of Engineering and Technology, King Mongkut's University of Technology North Bangkok (Rayong Campus), Thailand.

[d] Research and Development Center for Chemical Engineering Unit Operation and Catalyst Design (RCC), 1st and 7th floor (Room 702), STRI Building, King Mongkut's University of Technology North Bangkok, Thailand.

[e] Process and Systems Engineering Center (PROSYS), Department of Chemical and Biochemical Engineering, Technical University of Denmark, Søltofts Plads Buildings 227 and 229, 2800 Kongens. Lyngby, Denmark.

*Corresponding Author 19 Moo 11 Tambon Nonglalok, Amphur Bankhai, Rayong 21120, Thailand.
Tel: (+6638) – 627 – 000 Ext. 2300, Mobile: (+6680) – 044 – 9344
E-mail: piyapong.h@eat.kmutnb.ac.th (P. Hunpinyo)

Manuscript submission for consideration for possible publication in Chemical Engineering Research and Design (SI: Energy System Engineering)

Abstract

Due to the irregular nature of solar resource, solar photovoltaic (PV) system alone cannot satisfy load on a 24/7 demand basis, especially with increasing regional population in developing countries such as Thailand. A hybrid solar PV/biomass based along with battery storage system has been drawing more attention to option since it promises great deal of challenges and opportunities for different rural areas. Thailand rich with higher level of agricultural crops and biomass materials, is a prospective candidate for deployment of bio-power to complement such hybrid systems. To this end, in this study a customized hybrid power system integrating solar, biomass (syngas) power and battery storage system is evaluated a pilot scale for micro off-grid application. This paper shows that for a reliability of a hybrid syngas/solar PV system along with rechargeable batteries, the syngas generator can guarantee a continuous 24 hours electricity supply in case of shortage of energy (during on cloudy day and at the nighttime). Two consecutive days of commissioning phase are necessary for the entire system to operate, which is a solid basis for including the syngas generator in the hybrid system. Furthermore, the generator has to be always synchronized during the commissioning time. Battery state of charge (SOC) in percent (%) connecting with syngas is greater than solar PV and the charging time appears significantly shorter than that one. All possible combinations between an innovation and existing systems can serve as a guideline for making similar studies in the context of different off-grid sites and more. Next, optimal scale up and design of hybrid power system for different off grid applications will be performed including comprehensive uncertainty analysis to facilitate robust and renewable electricity generation.

Keywords: Torrefied rubber wood, Modified downdraft gasifier, Syngas, Internal combustion (IC) engine, Hybrid solar PV/syngas/battery system, Thailand

Nomenclature

LHV	low heating value	[MJ/kg or MJ/m^3]
HHV	high heating value	[MJ/kg or MJ/m^3]
m	mass flowrate	[kg/h or m^3/h]
n	revolutions per minute	[r.p.m]
CCE	carbon conversion efficiency	[%]
CGE	cold gas efficiency	[%]
V_g	total volume of syngas	[Nm^3/h]
Y_{gas}	dry gas yield	[Nm^3/kg]
W_{moist}	weight fraction of biomass moisture	[%wt]
BTDC	before top dead center	[degree]
kWp	kilowatt peak	
SOC	state of charge	[%]
IC	Internal Combustion	
ASTM	American Society for Testing and Materials	
ASME	American Society of Mechanical Engineers	

Subscript

moist	moisture
ref	reference

Greek symbols

67	η	efficiency
68	λ	air to fuel mixture
69	φ	equivalence ratio

1. Introduction

About 60% of the Thailand population lives in the rural areas, and around 12% of the rural households i.e., most living in small remote villages and isolated islands still lack access to grid electricity (Network 2015). Obviously, higher electricity line expenses, transmission and distribution losses (T&D losses) and the large infrastructure required for regular O&M make the rural electrification through conventional grid extension an economically unattractive option for the remote areas (Rajbongshi, Borgohain et al. 2017). Also, a utility grid extension for grid connected main system is infeasible administratively due to such conditions as dispersed people and obstacle operation (IEA 2011; Mainali and Silveira 2013). Recently, the Thai's government has set the target of raising the access rate to the reliable, grid-quality and affordable prices electricity services to 80% of the rural households by the year 2025 (IEA 2016). The Government aims to provide electricity to un-electrified villages through renewable energy applications. This has drawn extensive public attention to the need of off-grid system on a stand-alone power system (SAPS) from renewable energy systems (RESs) such as solar photovoltaics (PV) power in many regions. In fact, solar energy is regarded as a clean, climate-friendly, abundant energy resource, and with cost-effective characteristics (decreasing cost of PVs). This makes PVs among the likely viable energy supply solutions to such rural areas (Salas, Suponthana et al. 2015).

However, the techniques and smart methods for more efficient solar performance are still evolving. A major disadvantage of solar power is its discontinuous and irregular (dependency on weather conditions) nature – the sun doesn't shine 24 hours a day. When the sun goes down or is heavily shaded until night falls, solar PV panels stop producing electricity. Likewise the energy yield of solar panels decreases on cloudy or foggy days since less sunlight can pass through the clouds to reach solar panels; however,

these weather conditions do not mean that no electric power is produced – just a lot less (Yamegueu, Azoumah et al. 2011). The risk factor of energy supply is mainly due to dependence on sunshine hours which are changeable. As a matter of fact, the solar irradiance levels and the electricity demand time distributions do not match. It is therefore necessary to consider other renewable energy sources in order to enhance the energy availability and security situation in Thailand.

The concept of a hybrid power system depends on many factors. One of the alternative solutions for addressing these above challenges would be a hybrid solar PV system which combines two energy sources with a variable output. An appropriate choice of innovative technology for the additional energy sources should consider the following criteria: ability to utilize diverse fuel sources, emissions reductions (climate friendliness), and efficiencies. Furthermore, combining the two sources of solar and another thing can provide better reliability and their hybrid system becomes more economical to operate since the weakness of one system can be complemented by the strength of the other one.

In rural areas of the Southeast Asian countries like Thailand, around 80% of people still use agricultural biomass wastes into solid charcoal and residual woody for their energy need (Pode, Diouf et al. 2015; Samiran, Jaafar et al. 2016). Advancement in the biomass-to-energy conversion technologies has revived interest in the use of these feedstock because of its renewable and carbon–neutral nature. Among these conversion technologies, biomass-derived syngas gasification is the most reliable and can be converted into many forms such as heat, electricity and bio-fuels (Hagos, Aziz et al. 2014; Hunpinyo, Cheali et al. 2014). Due to the electricity production in biomass gasification technology, producer gas can be used directly as fuel in a spark ignition internal combustion (IC) engine coupled with a generator set (or called genset) (Reed, Das et al. 1988; Lv, Xiong et al. 2004; Hsi, Wang et al. 2008; Basu 2010).

A modified engine-generator set plays a major role in the distributed power generation for an electric output requirement (Fanelli, Viggiano et al. 2014). It has very durable, versatile and flexible applications in moving and stationary machineries. Compared to different fuel types of combustion technologies, syngas genset is believed to have benefits like low capital cost (Singh and Baredar 2016; Singh, Singh et al. 2016), reliability, easy access to their required spare parts, easier operating system and control, and modularity (Lieuwen, Yang et al. 2009). A combustion engine system is convenient to use devices without technical supervision, especially in remote villages and rural communities, located in mountainous areas isolated from the main electric grid. In addition, the introduction of syngas utilization decreases the dependency on fossil fuels. This is where syngas engine-generator set is expected to be complementary to the intermittent nature of solar electric energy. Electricity generated by genset can also be connected independently on the primary function of storage batteries to guarantee a continuous 24 hours supply for small off-grid systems. Therefore, the key challenges of design and operation for hybrid power stations includes the following: a suitable replacement of fossil fuels by syngas fuels and improvement of efficiency for solar energy during at night and on cloudy days and optimal combination with respect to economics and robustness of different components of hybrid system**.**

To the best of authors knowledge, none of the researchers have worked on the innovation design and operational system of a hybrid syngas/solar PV along with the battery storage in actual off-grid situation, to fulfill the electrical demand of a typical village. Almost all researchers focused on cost of energy (COE) production and optimum size with the support of the HOMER software simulator hybrid optimization model for electric renewable. In the existing literature, several hybrid systems are simulated through solar PV/ biomass without storage (Bhattacharjee and Dey 2014), solar PV/ biomass with battery

134 energy storage (Harish Kumar 2013; Pradhan 2013; N. 2014; Singh and Baredar 2016; Singh, Singh et
135 al. 2016), solar PV/ biomass/diesel with battery energy storage (Rajbongshi, Borgohain et al. 2017).

136 For instance, (Bhattacharjee and Dey 2014) proposed a PV-biomass hybrid system for isolated areas of
137 India. The authors carried out economic analysis and component selection with the help of the standard
138 software tool hybrid optimization model for rural electrification. (Harish Kumar 2013; N. 2014)
139 proposed a PV-biomass based hybrid system for a location in New Zealand. The system sizing was
140 obtained with the help of HOMER. (Pradhan, Bhuyan et al. 2013) evaluated a PV-biomass hybrid
141 system for rural electrification on the basis of levelized cost of electricity (LCOE). To design hybrid
142 system a mixed integer linear programming based model has been developed, (Singh and Baredar 2016;
143 Singh, Singh et al. 2016) integrated solar and biomass resources to develop a mathematical model of an
144 autonomous PV-biomass energy system with battery bank to provide electricity for an off-grid location.
145 The main contribution is to compare the performance of the applied simulation technique on a large
146 scale, the results achieved by the artificial bee colony (ABC) algorithm have been compared with
147 particle swarm optimization (PSO) and HOMER programs. It has been verified from the results that the
148 proposed hybrid system is able to manage a smooth power flow with the same optimal configuration.
149 (Rajbongshi, Borgohain et al. 2017) presented electrical cost analysis of hybrid PV-biomass-diesel
150 energy system for comparing between grid extension and off-grid hybrid energy system in 100
151 households located on the north zone of India using tool HOMER. It is inferred from the simulation
152 results that biomass gasification system could play an important role and the best option in energy
153 generation, particularly in rural areas.

154 The main objective of this paper is to test and demonstrate on a pilot scale reliability and stability of the
155 proposed hybrid solar PV/biomass system with battery energy storage to supply electricity under

different electrical load demand during the day. The outcome of this demonstration is indeed important to provide the local decision-makers (who have enough agricultural biomass resources) with the existing solar PV facilities to consider replacement of fossil fuels for continuous electricity supply for off grid applications. The manuscript is structured as follows: First the hybrid power is system presented and then the principle governing the design, configurations and operational strategies of different components of are explained in detail. A special focus is given on the section of biomass gasification via generator set to guarantee a continuous 24 hours electricity supply. Next the results are presented, critically analyzed and discussed. Conclusion section outlines main findings and future perspectives from this study.

2. Proposed hybrid solar PV/syngas system in Thailand

2.1 Hybrid solar PV/diesel generator system by utilizing syngas as fuel

Currently, many remote areas of Thailand are found to be used both generators and solar PV panels for producing electricity. Namely, diesel generators help power applications many aspects of both prime and standby. Most people live in almost total darkness depend on diesel/gasoline fuels to provide electricity in their rural villages where connecting to the main grid is not possible and generators also help to overcome issues associated with unreliable, outdated and non-existent electricity grids.

The majority of commercially-available generators are designed to run on fossil fuels and they have some major disadvantages and limitations. First, the fuel consumptions are non-linear related to load ratio, namely, it has low efficiency at low load demand in order to increase more levelized costs of electricity and high price fuel, including the logistical problem of transporting the diesel fuel to remote areas. Second, Emission levels of diesel fuel after burning IC engine such as NO_x, carbon monoxide

(CO), hydrocarbons, and particulate matter are produced as a substantial contributor to poor air quality in the surrounding environment (Kumar, Khare et al. 2015).

Alternatively in this hybrid system, a new equipment is used to allow the genset to be fed with biomass-based syngas. The operation of fuel injection system on syngas has been adopted in many provincial regions in Thailand and this change has similar performance as diesel engine at 1500 rpm of speed.

2.2 Dispatch strategy of proposed hybrid system

The schematic operation of hybrid syngas/solar/battery system is illustrated in **Fig. 1**. The issue of dispatch strategy is planned and designed as following on two scenarios: in normal operating situation (see **Fig. 1a**), solar PV provides the load demand during the daytime (around 07.00 a.m. to 19.00 p.m.) during the winter and summer months. The excess energy (the energy above the average hourly demand; if any) from the PV panels is charged in the lithium battery until 70% (an initial set-point) or more of full capacity of the battery status. As shown in **Fig. 1b**, a standby syngas genset system is brought-on-line on cloudy days and during at the nighttime (around 19.00 p.m. to 07.00 a.m.) when solar PV fails to satisfy the load designed and once the level of battery storage (see **Fig. 1c**) has been depleted. This means is that the syngas genset is used for a backup power system. A self-regulation control system is started at full capacity when the battery's SOC is lower than 40% minimum required and it still runs continuously until the battery reaches a specified charge level of 80% and then it shuts down automatically.

****

Fig. 1 Dispatch strategy of hybrid syngas/solar/battery system through off-grid bi-directional inverter: on two scenarios (a) the excess energy, (b) and (c) the shortage energy.

****

198

199 **3. Materials and methods**

200 The components of the proposed hybrid system are detailed below including collection and recording of
201 the main data for performance analysis. The hybrid power station consists of biomass resource and
202 gasification, syngas genset, solar system components, batteries and electric loads.

203 3.1 Biomass feedstock and properties

204 The typical biomass uses for the proposed system came from the furniture factories in Rayong province.
205 Some amounts of waste rubber-wood-sawdust were torrefied pellets which is an efficient form to store
206 and transport biomass based fuel source Thus, samples of torrefied wood pellet (see **Fig. 2**) have been
207 selected as the feed material for this study. Notice, the calorific value of the biomass fuel feeding the
208 gasifier should not be less than 9 MJ/kg (Elsner, Wysocki et al. 2017). The length size of pellets should
209 be between 40 mm and 100 mm in order to ensure enough the void (i.e. "empty") spaces in a bed for the
210 gasification process as well as to give the heat transfer from the throat zone upwards. The lower limit
211 constraint on pellet size (40 mm) is increased the pressure drop within the fixed bed at a reasonable
212 level. It has been confirmed experimentally (Mayerhofer, Govaerts et al. 2011) and numerically (Marek
213 2017) that the particle diameter directly effects the pressure drop in fixed beds. The biomass gasification
214 system is tested with torrefied rubber wood pellets with a moisture content of approximately 6% wt. (dry
215 basis). The biomass ash and moisture levels should not exceed 5% wt. and 20% wt. (Elsner, Wysocki et
216 al. 2017). The chemical characterization of the local torrefied rubber wood used in this study is presented
217 in **Table 1**. In particular, torrefied rubber wood pellets are characterized as ASTM standard test method

through proximate analysis (Thermogravimetric method), ultimate analysis (providing the elemental composition of the sample) and calorimetric analysis (for the heating value), respectively.

****

Fig. 2 Torrefied rubber wood pellet used for gasification. Pellets are 10 mm diameter cylinders of average 50–150 mm length.

****

****

Table 1 Chemical characterization of local torrefied rubber wood tested in gasifier.

****

3.2 Modified air-downdraft gasifier and syngas compositions

The modified gasifier used in this research is a compact scale that was designed and built in the King's Mongkut University of Technology North Bangkok (Rayong campus) cooperated with Alternative Energy System Co,.Ltd (Co-founder), all parts are fabricated as following on ASME pressure vessel code (Boiler and Committee 1997; Rao 2009). The internal volume is capable of at least approximately 40 kg/h up to 50 kg/h for feeding an opening top. Schematic diagrams with a typical temperature profile and the whole zones are shown in **Fig. 3**. In general, hardware of the experimental system essentially consists of a downdraft gasifier, tar condenser and trap, bag filter drum, electric vacuum blower (axial fan) and a flare pipe. This gasifier has four distinct reaction zones, which are drying feedstock (or called condensing zone), pyrolysis (or called drying zone), oxidation and reduction zones from top to bottom (height of the total bed (H) = 1350 mm, internal diameter (ID) of the oxidation zone (D) = 300 mm, ID of the drying hopper zone (L) = 300 mm, ID of the throat (d) = 280 mm). Principle of operation is a semi-batch modified downdraft reactor using atmospheric air as oxidizing agent. Inner chamber of both reduction and combustion zones made of stainless steel grade 253MA to secure the oxidation at higher

reaction temperature. In parts of the fabrication, the entries configurations are consist of a fuel hopper, a gasifier reaction zone, air feeding devices (filter and rota-meter) integrated a recuperator box, and an ash removal chamber. For the process control unit (PCU), five K-type thermocouples are installed to display temperature profiles in the middle of each significant zone. The vacuum blower installed after the filter tank is varied speed by an inverter and an oxygen sensor is introduced to regulate automatically the blower frequency. During burning biomass, the grate shaker lies below the reduction zone is controlled relatively with the pressure ratio across the reactor to shake the grate for a given shake time and interval. All electric and signal devices are monitored and controlled by a commercial software, realized in LabView environment.

****

Fig. 3 Schematic diagram of modified downdraft reactor (approximately 40-50 kg/h) and its typical temperature profile through gasifier during operation

****

The first zone, or uppermost, this zone receives pellet fuel from the top that is dried and evaporated moisture in the air circulated through the first zone. In the case of vaporization of moisture until liquid droplet through the top cover is removed by sloping trough. The second drying zone gets heat delivery from the third zone principally by thermal conduction. The heat builds up into the pellet woody (see zone III in Fig 3). Around 400 ºC, it starts to undergo pyrolysis condition which the woody fuel is forced to decompose into a variety of substances - one of them being charcoal, non-condensable gases as a producer gas (CO, H_2, CH_4, CO_2, N_2 and H_2O), and tar vapors (condensable gases). One of the main advantages of this design, most of the tar is cracked and the char is gasified in this zone, where hot air is injected through surround 6 nozzles along with the feed. Excess oxygen in front of the 6 nozzles facilitates combustion (or called oxidation) of part of the char and creating a very high temperature at

1,000ºC. The volatiles consist mainly of carbon monoxide and hydrogen, and may include a variety of other hydrocarbons and some fly ash exits from the bottom side of the reduction zone. Heat release from the combustion zone is conducted turnaround the gasifying zone, so the air stream pass through the hot syngas exiting the reactor to heat up the incoming air while cooling the syngas. The syngas consists mainly of carbon monoxide and hydrogen exiting the reduction zone first passes through a hot trap, where some of the soot and most of the fly ash is collected, cooled down in tube condenser, and bag filter, respectively.

Due to performance testing, both fresh air inlet and syngas effluent streams are regulated using variable speed drive (VSD) on air vacuum blower to allow a narrow range of air/fuel ratio (lambda, λ) values for acceptable syngas quality. Stable gasifier operation of the gas quality produced is in the range of 106 ± 2 Nm^3/h at standard pressure and standard temperature. Gas composition data is collected to analyze using a chromatograph type GC-MS system Agilent Technologies 7890. The sampling of tars is determined by using standardized methodology as followed in regulations for the Tar protocol (Lee, Speight et al. 2014).

To achieve the gasification performance, there are a number of factors at least five parameters can be defined to assess the fabrication and installation including its reliability, stability of operating process, and more importantly the energy conversion efficiency. To solve for substituting, the given information in all equations are displayed separately in **Supplementary Data Appendix A**.

a) The equivalence ratio, ER (φ) of gasified biomass for each run is calculated by Eq. (1) (Reed, Das et al. 1988).

$$ER\ (\varphi) = \left.\frac{Air\ flow\ rate}{Biomass\ consumption\ rate}\right|_{Actual} / \left.\left(\frac{Air\ flow\ rate}{Biomass\ consumption\ rate}\right)\right|_{Stoichiometric} \quad \text{Eq. (1)}$$

where air/biomass fuel ratio for stoichiometry equals 1 is 5.22 m^3 of air/kg of torrefied wood pellets. The ER obtained by using Eq. (1) was found to be in the range of 0.25–0.4 (Ashok Jayawant Rao KECHE 2013).

b) Carbon conversion efficiency (CCE), η_{cce} (%) can be applied by Eq. (2) (Lv, Xiong et al. 2004; Sattar, Leeke et al. 2014; Materazzi, Lettieri et al. 2016),

$$\eta_{CCE} = \frac{\dot{v}_{syngas} \times 1,000 \times [CO\% + CH_4\% + CO_2\%] \times (12/22.4)}{W \times (1 - X_{ash}) \times C\%} \times 100\% \quad \text{Eq. (2)}$$

where CO%, CH_4%, and CO_2% are the gas concentrations as a volume fraction and $\dot{v}_{syngas}$ (Nm^3/h) is the total volumetric flowrate of dry gas produced at STP condition, W is the dry biomass feeding rate (g/h), X_{ash} is the ash content in the feed, and C% is the carbon content in the ultimate analysis of biomass.

c) For direct syngas combustion after the gasifier, hot syngas sensible heat has to be considered to the chemical power in the gas efficiency calculations. The cold gas efficiency (CGE) of gasifier can be determined as follows:

$$\eta_{CGE} = \frac{\dot{v}_{syngas}\left(Nm^3/hr\right) \times LHV_{syngas}\left(MJ/Nm^3\right)}{\dot{m}_{biomass}\left(kg/hr\right) \times LHV_{biomass}\left(MJ/kg\right)} \times 100\% \quad \text{Eq. (3)}$$

298 In above relation $\dot{m}_{biomass}$ represents the biomass loading (kg/hr), $LHV_{biomass}$ stands for the calorific value

299 of a biomass (MJ/kg), and $\dot{v}_{syngas}$ $(\mathrm{Nm}^3/\mathrm{h})$ and $LHV_{syngas}(\mathrm{MJ}/\mathrm{Nm}^3)$ are the generated syngas

300 volumetric flowrate at STP condition and its calorific value, respectively.

301 d) Dry gas yield (Nm^3/kg), The applied relation is: (Sattar, Leeke et al. 2014)

302 $$\mathrm{Y}_{gas} = \frac{\dot{v}_{syngas}\left(Nm^3/h\right)}{(1-\mathrm{W}_{\mathrm{moist}})\times m_{biomass}\left(kg/h\right)} \qquad \text{Eq. (4)}$$

303 where $\dot{v}_{syngas}$ is the total volumetric flowrate (Nm^3/h) of gas produced during gasification calculated from

304 the nitrogen balance, considering that nitrogen in biomass is negligible, $\mathrm{W}_{\mathrm{moist}}$ is the biomass percent

305 moisture by weight fraction w/w %).

306 e) The dry product gas low heating value, LHV (MJ/Nm^3) for the biomass producer gas has been

307 calculated as follows (Klein and Nellis 2011):

308 $$LHV = \left[\left(0.126\times C_{CO}\right)+\left(0.10794\times C_{H_2}\right)+\left(0.3505\times C_{CH_4}\right)\right] \qquad \text{Eq. (5)}$$

309 where three typical compositions of CO, H_2, and CH_4 are the gas concentrations of the producer gas.

310 3.3 Modified gas engine/generator set

311 Schematic of biomass gasification coupled to an IC engine for electricity generation employed in this
312 work is depicted in **Supplementary Data Appendix B**. A pickup truck engine specifications, Made in
313 Japan (ISUZU model 4BC2), are also listed in **Table 2**. The engine capacity is chosen coincident with
314 the minimal syngas flowrate requirement and should be related with the swept volume of all the pistons
315 inside the cylinders of a reciprocating engine. Without increasing the knocking tendency, the in-line
316 four-cylinder engine plays an overall displacement volume of 3.3 L by installing both turbocharger air
317 intake and intercooler systems. The fuel injection system is designed on a direct injection diesel engine
318 that it is modified and coupled with a 50 Hz electric generator. The internal combustion system has been
319 equipped originally with a carburetor, which is removed and replaced with a new intake manifold and
320 lean burn syngas fuelled spark ignition.

321 **********
322 **Table 2** Overall performances of a modified genset fuelled with torrefied rubber wood syngas
323 **********

324 3.3.1 Description of gas engine configurations

325 In order to avoid increasing the knocking tendency (Lapuerta, Hernández et al. 2001), an ignition system
326 is achieved at a compression ratio of 11.5:1 using a spark plug installed at both directionality and angle
327 degree (28º BTDC) for injecting a gaseous fuel (Przybyla, Szlek et al. 2016). It is noted that the ignition
328 timing for conventional spark ignition engines fueled with gasoline vary between 10º and 40º degree
329 before top dead center (Heywood 1988). The pressure of the air/fuel mixture is boosted by a
330 turbocharger installed in the intake system, which had a maximum boost pressure of 1.5 bar. The
331 maximum power output of a generator linked to the engine is 45 kVA. Once a lower rotation speed
332 engine is a condition required for syngas application, a digital governor is programmed to limit engine

333 speed and to control the throttle valve for regulating the syngas flow according to the operating load, and
334 hence maintaining the desired engine speed.

335 3.3.2 Description of gas engine/generator control system

336 Through all the trials, the syngas engine/generator (genset) system is rotated at fixed speed of 1500 rpm
337 in order to comply with the required electric power frequency of 50 Hz. The modified engine is fed with
338 a stoichiometric air/fuel mixture ratio (through lambda sensor), with fuel being a substitute syngas
339 supplied from a pressurized cylindrical tank. With this signal, the process control unit and control logic
340 adjust from the lean or rich mixture to the proper air to syngas fuel ratio through PID control. A P&ID of
341 the proposed biomass-to-electricity system is shown in **Fig. 4**. The overall process efficiency of biomass
342 air gasification-generator set can be defined as following below. The solution of efficiency equations are
343 substituted and arranged in **Supplementary Data Appendix A**.

344 The overall process efficiency of biomass air gasification-generator set can be defined as follows:

345 $$\eta_{overall} = \frac{P_{electrical\ output}\,(kW) + H_{useful\ heat\ output}\,(kW)}{\dot{m}_{biomass}\left(\frac{kg}{hr}\right)\times LHV_{biomass}\left(\frac{MJ}{kg}\right)\times\left(\frac{1}{3,600}\frac{h}{sec}\right)\times\left(\frac{1,000}{1}\frac{kJ}{MJ}\right)}\times 100\% \qquad \text{Eq. (6)}$$

346 The efficiency of gas engine can be determined as follows:

347 $$\eta_{engine} = \frac{P_{electrical\ output}\,(kW)}{\dot{v}_{syngas}\left(\frac{Nm^3}{h}\right)\times LHV_{syngas}\left(\frac{MJ}{Nm^3}\right)\times\left(\frac{1}{3,600}\frac{h}{sec}\right)\times\left(\frac{1,000}{1}\frac{kJ}{MJ}\right)}\times 100\% \qquad \text{Eq. (7)}$$

348 The electrical efficiency can be determined as follows:

$$\eta_{electricity} = \frac{P_{electrical\ output}\ (kW)}{\dot{m}_{biomass}\left(\frac{kg}{hr}\right) \times LHV_{biomass}\left(\frac{MJ}{kg}\right) \times \left(\frac{1}{3,600}\frac{h}{sec}\right) \times \left(\frac{1,000}{1}\frac{kJ}{MJ}\right)} \times 100\% \quad \text{Eq. (8)}$$

The power station efficiency can be determined as follows:

$$\eta_{power} = \frac{P_{net\ electrical\ output\ serves\ the\ load}\ (kW)}{\dot{m}_{biomass}\left(\frac{kg}{h}\right) \times LHV_{biomass}\left(\frac{MJ}{kg}\right) \times \left(\frac{1}{3,600}\frac{h}{sec}\right) \times \left(\frac{1,000}{1}\frac{kJ}{MJ}\right)} \times 100\% \quad \text{Eq. (9)}$$

which the net electrical output serves the load refers to the whole electrical power minus the self-consumption power of the system

The thermal efficiency of system can be calculated as follows:

$$\eta_{thermal} = \frac{H_{useful\ heat\ output}\ (kW)}{\dot{m}_{biomass}\left(\frac{kg}{h}\right) \times LHV_{biomass}\left(\frac{MJ}{kg}\right) \times \left(\frac{1}{3,600}\frac{hr}{sec}\right) \times \left(\frac{1,000}{1}\frac{kJ}{MJ}\right)} \times 100\% \quad \text{Eq. (10)}$$

****

Fig. 4 Process and Instrument Diagram (P&ID) layout of the proposed biomass-fueled genset system connecting with the mass and energy balances

****

In a controlled manner, the Deep Sea Electronics (DSE) is installed to synchronize for the useful features of the switchgear application. Otherwise, the model DSE7420 module can be compatible with two magnetic speed pickup units (MPUs) and alternator sensing through the configuration suite personal computer (PC) tool program. Within this program, the settings and control dynamics can be changed

(target RPM, over speed threshold, PID controls, droop, automatic start/shutdown states, LED/LCD alarm indication and power monitoring (kWh and kVA). A heuristic method of tuning a PID controller in both engine and generator can watch directly in **Supplementary Data Appendix E.**

3.4 Solar PV system configurations

3.4.1. Solar panel module

The solar radiation information has a great effect on the continuous increase of the performance of solar PV system. This value can be related taking into consideration the tilting angle of solar arrays. Monthly averaged incident solar power in this area is quite high especially during in winter and summer from November 2016 to May, 2017, where it not exceeds 7.5 kWh/m^2/day on horizontal plane. Optimum tilt angle is set to be 15º (±2.5º). The sunlight can be directly converted into electric production by PV panels and arrays. The current output of a solar module relies a function of voltage and depends on solar radiation and temperature. The panel's power output can be found by multiplying the current (A) and the voltage (V). The panels are all re-deployed to power a total of 315 W x 39 modules, 97% efficient solar converters (each converter has its own 99.5% efficient maximum power point tracking, MPPT). As specified in Table C2 of **Supplementary Data Appendix C**, the method is involved with arranging on both 1st string of 6 panels and 2nd string of 7 panels in series. The power supplied by the solar PV panel is calculated by Eq. (11) and it can be given below (Daud and Ismail 2012),

$$P_{PV-DC\,out} = P_{N-PV} \times \left(G / G_{ref} \right) \times \left[1 + K_T \left(T_c - T_{c,\,ref} \right) \right] \qquad \text{Eq. (11)}$$

where $P_{PV-DC\,out}$ is output power (DC) from the PV arrays (kW)

384 P_{N-PV} is rated power (DC) at reference conditions (kW)

385 G is solar radiation (kW/m^2)

386 G_{ref} is solar radiation at reference conditions (G_{ref} = 1 kW/m^2) (Sukamongkol,

387 Chungpaibulpatana et al. 2002)

388 K_T is temperature coefficient of the maximum power $\left(1/^{\circ}C\right)$, where $K_T = -3.7\times10^{-3}$ for typical

389 Silicon material coating on solar panels

390 T_c is array (cell) temperature (ºC), which can be determined by

391 $T_c = T_{amb} + \left[\left(G/800\right)\times\left(NOCT - 20\right)\right]$ where T_{amb} is the ambient temperature (ºC) and the $NOCT$ refers

392 to a nominal operating cell temperature (ºC) that is given in all PV specification sheets from the

393 manufacturer, respectively.

394 $T_{c,ref}$ is array (cell) temperature at reference conditions ($T_{c,ref} = 25^{\circ}C$)

395 3.4.2 Solar PV arrays and inverters

396 An electric circuit diagram of a hybrid power system is depicted in **Fig. 5**. Initially, solar PV captures the

397 solar energy using PV arrays. When sunlight hits the panel DC current is generated. This DC current is

398 then fed into inverters to convert it to AC current for the primary load. Three solar PV inverters are

399 usually sized a little larger rating to the solar panels to an allowable size of 1.05 times the solar array

400 power rating and then it installed to act as interface between each of solar PV arrays and the bidirectional

401 inverters (BDIs). The excess PV electricity generated is sufficient to partially charge the battery through

402 the BDIs, it can be charged only during the daytime. The battery can reach 70% SOC before the twilight

403 period starts. The amount of this stored energy will be prepared to use later for supplying the next whole

nighttime. A standby syngas genset is only needed if the batteries need recharging in times of unfavourable weather or if loads exceed inverters capacity. Whilst the genset fueled by syngas is running it powers the loads and the BDIs operates as a powerful battery charger to replenish the batteries.

****

Fig. 5 Proposed electrical diagram of a hybrid syngas/solar PV /battery power system for off-grid applications

****

3.5 Bidirectional inverter

A BDI has two ports: AC and DC ports. Its function is essential to the hybrid off-grid system where both a battery storage system and a backup syngas genset are involved in the proposed system. BDI can transfer power simultaneously in both directions between the DC and AC segments. Namely, the BDI can supply DC side and charge the Lithium batteries therefore it can provide a path from the AC bus to the DC bus, in this case it acts as a full wave rectifier circuit which changes AC syngas genset voltage to DC voltage. In the other side, BDI can provide path from DC bus to the AC load therefore it acts as a functional inverter which changes from DC voltage to AC voltage needed by the designed load. The BDI has to be capable of controlling the maximum expected power of AC loads. Thus, it can be chosen 20% higher than the rated power of the summation of AC loads.

For the three phase connection (see **Fig. 5**), each phase is connected directly to the corresponding BDIs, where phase 1 is connected to the master unit, phase 2 is connected to slave 1 and phase 3 is connected to slave 2. The genset connections can be paralleled to three BDIs in order to deliver electrical power from the prime generator. The master BDI can synchronize with the standby genset to be compatible

with a built-in relay port through the function of switchgear. To use this common function, the backup genset can support the automatic startup functions. The standard signal wires of each connection point on a Deep Sea DSE7420 device from the standby genset are shown in **Supplementary Data Appendix D**. The available back solar PV power output after BDI (AC side) is dependent on the BDI efficiency (Ajan, Ahmed et al. 2003).

$$P_{out\ (Bi-inv)} = P_{in\ (Bi-inv)} \times \eta_{Bi-inv} \qquad \text{Eq. (12)}$$

where $P_{out\ (Bi-inv)}$ is the available solar PV power AC output (kW)

n_{inv} is the BDI efficiency, which is considered as 95%.

3.6 Lithium batteries charging/discharging station

As previously mentioned, solar PV system may not be able to meet the load demands at all times and is supposed to be running in a hybrid manner, cycling the batteries system (charging and discharge modes). Lithium batteries are designed to capture surplus electricity generated by solar PV system during daytime peak demand and allow itself to be stored solar electricity for use later. For low or no solar radiation, potentially batteries are planned systematically to use as a back-up power system and they are charged both independently and coincidentally with syngas genset when the battery SOC status is less than 40%. Its performance likewise keeps up consistent voltage over the electrical load. The total capacity required $\left(C_{kW}\right)$ for the assembly of batteries in a solar PV system can be computed by adopted from (Ajan, Ahmed et al. 2003; Singh and Baredar 2016).

$$C_{kW} = \left[\left(ED_{day} \times HD_{day}\right) + \left(ED_{night} \times HD_{night}\right)\right] \times \eta_{inv} \times \eta_{batt} \times DOD \qquad \text{Eq. (13)}$$

where ED_{day} is total energy demand available for storage for a day at daytime (kW)

ED_{night} is total energy demand available for storage for a day at nighttime (kW)

HD_{day} is hourly autonomy at daytime or the period of storage required (in hours)

HD_{night} is hourly autonomy at nighttime or the period of storage required (in hours)

n_{inv} is BDI efficiency (%),which is thought to be 95%

n_{batt} is Lithium battery efficiency (%),which is thought to be 95%

DOD is the maximum allowable depth of charging and discharging cycles (%), which is thought to be 60%-80%, depending on the manufacturer

However, the capacity of battery should be sized relatively with minimal hour allowable of a genset charging during the SOC reduction, especially voltage and current relationship.

4. Results and discussion

4.1 Mass balance of biomass gasification

The detailed mass input, mass output and the mass closure on the gasifier process are tabulated in **Table 3**, leads to examine the reliability of the results reported. Total mass input includes wood, fresh air with small moisture input and total mass outputs comprise of char, ash and syngas outputs. The char and ash are found in all units for the experiment, depending on their sizes. First place, some small particles of char and ash are vibrated by grate motor and falls into the bottom tray. Second, a wet dust is collected through condenser and finally some fine solid particles are filtered from bag filter in tank. All of them

464 are weighted and hence taken into consideration for data analysis. The mass balance closure is found to
465 be 95.07% for this experimental run (see in **Fig. 4**). For small-scale comparison, other studies report
466 material balances anywhere from 93% (Coronado, Yoshioka et al. 2011; Kotowicz, Sobolewski et al.
467 2013) to 98% (Pérez, Machin et al. 2015).

468 **********
469 **Table 3** The balance of mass streams on the combined thermal and power system (a) biomass air
470 gasification and (b) engine/generator
471 **********

472 **Table 3** reports the main air-downdraft gasifier performance indicating five significant parameters. The
473 operation of the dry gas yield is evaluated to be 2.82 Nm^3/kg at the ER value of 0.34. The gasifier
474 achieved operation efficiency with ER ranges of about 0.32-0.38, which is in a good agreement with the
475 optimum value for downdraft gasifier found by other researchers (Zainal, Rifau et al. 2002). The cold
476 gas efficiency (CGE) is calculated to be 59.85% and the carbon conversion efficiency (CCE) is found to
477 be 90.88% with specific biomass fuel consumption of 40.9 kg/h. The values appear to be quite consistent
478 with literature (Pérez, Machin et al. 2015; Patuzzi, Prando et al. 2016) at the same reactor size. A CGE
479 value between 60% and 65% indicates a moderate agreement level, while range of CCE value (90% −
480 95%) indicate substantial agreement level respectively.

481 As shown in **Table 4**, the results of the analysis of the gas sampled while running 3 hours of operating
482 timeframe has comparable to experimental results from (Jayah, Aye et al. 2003) that produced gas
483 compositions leaves from a proposed gasifier are not significantly different. Especially, a typical syngas
484 composition from biomass gasification in a downdraft reactor with air used as an oxidizing agent is
485 similar in the range of 15-20% of H_2, 15-20% of CO, 0.5-2% of CH_4, 10-15% of CO_2 and the other gas

is balanced by replacing N_2, O_2 and C_xH_y as previously reported by (Martínez, Mahkamov et al. 2012). For the present work, heating value of the syngas is characterized about calculating the LHV of 4.027 MJ/Nm^3 which is considered appropriate for combustion (Basu 2006). Its application as a suitable fuel in a modified IC engine has been confirmed also in a number of research set-ups in Denmark (Viking) (Ahrenfeldt, Thomsen et al. 2013), Finland (Volter) (Kaaresto, Ylikoski et al. 2013) and America (All power labs) (Przybyla, Szlek et al. 2016).

****

Table 4 Main gasifier performance parameters

****

4.2 Syngas and IC engine performance

The gasification efficiency is determined by **Eq. (3)** resulted in 59.85% for nitrogen-enrichment. Efficiency rate of a proposed air-blown gasifier is relatively good in value when compared with other values reported in the literature (Ahrenfeldt, Egsgaard et al. 2013; Ahrenfeldt, Thomsen et al. 2013; Gadsbøll, Thomsen et al. 2017; Thomsen, Sárossy et al. 2017). This reason could be interpreted by the proposed modification, that the increased temperature of the air influent stream in the recuperative preheater has directly affect key process variables like productivity and the calorific value of the producer gas. Moreover the successive reactions that comprise the decomposition, the Bounduard and the water shift reaction rates are taking place rapidly with the desired extent. It is worth noting that the LHV of producer gas reached 4.027 MJ/Nm^3 is still enough to ensure stable working conditions of the IC engine.

After finishing the load testing, the amount of tar formation has not been found prospectively in IC engine. This is also observed in (Elsner, Wysocki et al. 2017) study that increase in flow leads to higher temperature thereby avoid low level of tar formation. Principally, when the gasifier temperatures reach the target minimum temperature of 900 ºC, (> 1000 ºC ideally), tar content in the syngas may be low enough caused by thermal cracking before feeding into IC engine. Consequences of syngas operating in an IC engine, the revolution is kept constant at 1500 rpm and the compression ratio is to be 11.5:1 for a full load. The actual operation of the IC engine running on producer gas obtains a maximum electric power output of 33.7 kW. On average, biomass consumption is recorded at 40.9 kg/h. Summarizing, the observed performance (equivalencies) metrics are as follows: 1 kg of wood pellets 7.92% moisture content produces 2.82 Nm^3 of syngas and generates 0.82 kW electrical output, which this value is relatively fallen in the range of 0.75-1.86 kW/kg reported in the literature for modified diesel engines working with producer gas (Warren, Poulter et al. 1995; McKendry 2002; Products 2012; Röder, Whittaker et al. 2015).

4.3 Energetic analysis and electric power performance

In this section, the efficiencies related to electricity and heat production, internal losses, as well as the overall system efficiency for the biomass-to-electricity process are determined through the Equations (6) - (10). The energy efficiencies of different components are tabulated in **Table 5**. To make a better understanding of the energy flows of the proposed hybrid system, the proportion of the flow quality between the use of energy and losses in the entire process is balanced through Sankey diagram. Also, the relevancy and relative importance of the efficiency parameters involved in the entire system are estimated. A Sankey diagram of the energy flows in the integrated biomass gasification and engine/generator system is presented in **Fig. 6** and energy balance data is tabulated in **Supplementary**

Data Appendix C. Based on its lower heating value, the biomass energy flows are initially evaluated to be 198.8 kW. The chemical energy in biomass is transferred through the gasifier processor (i.e., air preheater, reactor, cooling and purification) and the IC engine to produce electricity and heat, with some losses. A small amount of energy is delivered at a low level with the assistance of warmed process air. The detailed percentage values with respect to the input energy of the biomass feedstock have been reported in **Table 6** for the proportion of losses, and thermal outputs and electrical production. On the exit side of the whole process, the largest energy proportion is contained in the thermal generation to be 43% (85.7 kW). It is apparent that heat loss during gasification is the second largest proportion, and this loss reaches approximately 40% (79.4 kW). For the proportion of electricity production, only 17% (33.7 kW) of the biomass feedstock is converted to net electricity, and 9.3 kW (4.7%) of the entire electricity production are shared for the self-consumption for the auxiliary equipment such as controller devices, compressors, motors in pumps and blowers etc. At second glance, 24.4 kW (12.3%) of the electricity left is sent to the load. The overall energy efficiency of the proposed system is approximately 44.21% as calculated in Eq. (6).

****

Table 5 Electricity, thermal and overall efficiencies for the proposed system

****

****

Fig. 6 A Sankey diagram of energy flows for the integrated biomass gasification and syngas genset systems

****

****

Table 6 Energy balance for the proportion of losses and thermal outputs and electrical production

****

552 4.4 A case study of Thailand

553 The selected proposed rural area of an educational institute, this location of the study area on the map
554 located off 12° 49' 40.6" N latitude and 101° 13' 06.1"E longitude. In **Fig. 7**, the best top view photo
555 taken with a drone, a stand-alone solar power system of 145 kWp was installed and being started up
556 since 2015. Only 12.3 kilowatt (kWp) of all energy is shared portion to join for the proposed hybrid
557 system. In this strategy solar energy is to serve the daily load which has required to use electrical
558 appliances like computers, televisions, tube and incandescent lights, ceiling fans, groundwater filtration
559 system and other machineries. The average daily load starts from 10:00 a.m. to 16:00 p.m. is
560 approximately 10 kWh which can be equivalent an electric source of illumination in 60 households.
561 Surplus electrical energy goes toward charging the battery bank. The data obtained from the
562 meteorological station displays a mean annual solar irradiation of 5.56 kWhr/m^2 per day for summer
563 period.

564 **********
565 **Fig. 7** The top view photo taken with a drone on the map located 12° 49' 40.6" N latitude and 101° 13'
566 06.1"E longitude (KMUTNB Rayong Campus) - a) 12.3 kWp of solar power separated to study for the
567 proposed hybrid system, b) Circuit breakers, c) PV inverters and d) Batteries storage
568 **********

569 The specification of different configurations of the proposed hybrid system such as solar PV array and
570 PV inverters, genset, BDIs and batteries have been presented on the conceptual design system used for
571 the selection criteria of all components as shown in **Supplementary Data Appendix C**. The sizing of
572 power system is relatively designed for 12.285 kW of solar panels, 12.6 kW of three converters, 33.7 kW
573 of a syngas genset, 13.8 kW of three BDIs and 60.9 kWh of battery capacity, respectively. The operating

574 schedule is tested to cover a period of two days. According to a comparative analysis of solar PV/battery
575 system, the graphical profiles without marking scale as depicted in **Fig. 8** have occurred predictably on
576 the real-time pattern. Solar PV current initially represents an orange line can generate so much electric
577 power during a first sunny day between 09:00-16.00 hours that it is significantly higher than AC
578 electricity demand (pink line). The excess solar PV generation unused immediately is conserved into the
579 energy storage. During the same period, the SOC of the battery bank (green line) witnesses a slowly
580 increase near its maximum allowable value from 43% to 68% in the usual time (approximately in 7-8
581 hours). A purple line confirms the battery current level with positive value (absorbing power) for
582 charging status. Consequently, only storage 68% of its remaining capacity aspects to be served the
583 electrical use during the next 1st nighttime for illumination requirements. The predicable circuit current
584 of a battery during discharge (releasing power) has been a downward trend to be negative between
585 19:00-07:00 hours. The trend lines of 2nd day remain the same situation.

586 One of the main concerns when implementing a solar PV/battery system without a standby genset is the
587 uncertainty of sunshine in the next 2nd daytime. When there are a lot of clouds in the sky or rainy, solar
588 panel efficiency drops as well as SOC may reduce ramp-down with increasing the daily load demand. In
589 order to deficit power spending, outage and blackout events may last from a few hours to a few days
590 depending on the irradiation of the sunshine hours, however the reliability of this system is difficult to
591 recover from quickly. Perhaps to solve for the above problem by offering a suggestion, the addition of
592 battery storage may extend its power outage compared to the existing one, however the main cause of
593 unstable system on consideration still depends on sunshine duration. Thus, the addition of a battery may
594 not prevent exactly a power failure problem and made many costly investments.

595 **********
596 **Fig. 8** Power profiles of a hybrid solar PV/battery system without a standby syngas genset
597 **********

598 In the case of the integrated syngas system, gaseous fuelled in a modified IC engine coupling generator
599 is synchronized to be running in a hybrid manner. Because of the fluctuating available of solar
600 irradiation, a wondering issue about insufficient power supply on cloudy days or at nighttime of
601 solar/battery system is solved to secure and reliable operation at all times. The syngas-to-power can be
602 synchronized seamlessly to hybrid solar PV/battery system for backup electric generation. The deficient
603 power generated by solar PV arrays can then be complemented at sudden time when the battery level
604 drops while discharging. One day before switching to syngas genset, the cleaned syngas effluent was
605 prepared in a gas storage tank (as shown in **Supplementary Data Appendix B**) which was typically
606 located separately to the main gasifier unit. The gas storage tank acts as a buffer in order to balance
607 fluctuations in the production of gas in the gasification process. Afterward the syngas was let to flow
608 into the receiver of gas holder, which from here was ready to be compressed into the syngas container
609 until reach approximately 10 bar gauge. The storage capacity of the syngas network is more than 140
610 kWh (24.4 kW x 6 h) which is large enough to supply for one week at a standby status. When syngas
611 production levels are highly variable, dual fuel mixing can be used to supplement the syngas with
612 liquefied petroleum gas (LPG).

613 When SOC dropped below 40%, the syngas genset was automatically started to be warming up at about
614 5 min of continuous idle operation (900 rpm). The air-fuel mixture under lean-burn conditions was
615 adjusted by a control box until the genset run stably. According to **Fig. B4** in **Supplementary Data**
616 **Appendix B**, the solenoid operated butterfly valve (CV-01) that will open by programming mechanism

was installed to arrange the flow of the syngas. Together with syngas, the fresh air was flowed through CV-02 into the mixer, and directed in to the electronic hydraulic actuator of the combustion chamber. It should be noted here that during starting the genset, the flow rate of the syngas was let maximum and reduce the rate until the genset start running. After that, the genset was accelerated at the synchronous speed of 1500 rpm (frequency 50 Hz and voltage range 380-415 V). Once the SOC was reached its target point, the genset automatically shuts.

At the beginning of the first night time between 03:00 - 06:00 hours (see in **Fig. 9**), the genset could be proven to operate seamlessly with smoothing in a charge scheduling. The time setting of the standby operation based triggering of the central controller is started automatically when the SOC level is lower than 40% and its application is capable of fixing complement in all seasons, with twenty-four hours of electricity supply, the different aspects of sunlight, quantity, quality and duration are not necessary to worry. In addition the percent of SOC level connecting with genset is greater than solar PV and the charge time appears approximately shorter than that one. This behavior may cause using higher voltage to transmit power and lower of amps rating between the batteries and the genset. Summary, the implementing results are capable to deliver an eminently suitable system and an appropriate strategy for the biopower development of this renewable sector, lead to give a novel idea of the performance on hybrid system available and identifying a possible way for improvement in the future.

****

Fig. 9 Power profiles of a hybrid solar PV/battery system with a standby syngas genset

****

Another major benefit is the replacement of average diesel use of 275 liters per month in supplying electricity at the same load and the corresponding reduction of CO_2 emissions gained (see calculation in

Supplementary Data Appendix F). One liter of diesel fuel can produce about 2.65 kg of carbon dioxide (Hazrat, Rasul et al. 2015). On a rough calculation at the same total displacement volume and the same total power produced within the cylinders, 8.748 tCO_2 emissions is prevented for a year thanks the use of renewable biomass source. However the assessment of economic feasibility of the entire syngas/solar PV/battery hybrid system based on financial indicators such as cost of energy (COE), net present value (NPV), internal rate of return (IRR) and time of return on investment (TRI) (payback period) as well as comprehensive sensitivity and uncertainty analysis will be further studied to further improve the technology readiness of the proposed hybrid renewable power system.

5. Conclusions

This study performs a pilot scale evaluation of the potential of a hybrid solar PV/biomass system with battery energy storage to serve with the electrical load demand at night or on cloudy days. In the propose hybrid power system two sources of renewable energy is combined: solar PV and biomass-derived syngas gasification via modified engine/generator set is synchronized to guarantee a continuous 24 hours supply for small off-grid systems. From the experimental results, the low heating value of the syngas resulted in 4.027 MJ/Nm^3. The engine's electrical output efficiency using a 100% of syngas resulted in 17% at maximum load. Considering a mechanical-to-electric power conversion efficiency of 95%, the maximum efficiency of the modified gas engine works out to be 28.2%. The thermal efficiency of the proposed biopower system was 16.9%, reaching an overall efficiency of 34.3%. The gasifier efficiency was 61.2%. Finally, the specific fuel consumption (torrefied rubber wood at 7.92% moisture content) for power generation using the ICE fueled with syngas equaled 1.21 kg/kWh and the specific fuel consumption (syngas) was 3.14 Nm^3/kWh.

The sizing of the proposed hybrid system is based on the following design basis 12.285 kW of solar panels, 12 kW of three converters, 33.7 kW of a syngas genset, 13.8 kW of three BDIs and 60.9 kWh of battery capacity, respectively. For each curve, at the first day of commissioning, the solar harvest has a sufficient possibility in responding to daily load fluctuations and being shared with power surplus on average charging for over 6-7 hours per day, while the syngas genset is capable of complementing the discontinuous nature of solar energy for standby power and back-up source under shorter charge time. The pilot scale testing results showed promising potential, which will be further studied for optimization and effective scale up for robust and economic off grid applications.

Acknowledgements

This work is part of the project for early stage design and synthesis of biorefinery (Grant No. KMUTNB-60-ART-109) supported by the research and publication funding of King Mongkut's University of Technology North Bangkok (KMUTNB). The authors would like to thank the research grant support by the National Research Council of Thailand (NRCT) under both grant number 224616 and proposal number 2559A11902041 since 2016. Finally, we would like to give special thanks to the Alternative Energy System (Thailand) Co, .Ltd. (www.alensys.co.th) where is a key partnership with innovation expert for designing a modern downdraft gasifier.

676

677 **References**

678 Ahrenfeldt, J., H. Egsgaard, et al. (2013). "The influence of partial oxidation mechanisms on tar
679 destruction in TwoStage biomass gasification." Fuel **112**: 662-680.
680 Ahrenfeldt, J., T. P. Thomsen, et al. (2013). "Biomass gasification cogeneration – A review of state of
681 the art technology and near future perspectives." Applied Thermal Engineering **50**(2): 1407-
682 1417.
683 Ajan, C. W., S. S. Ahmed, et al. (2003). "On the policy of photovoltaic and diesel generation mix for an
684 off-grid site: East Malaysian perspectives." Solar Energy **74**(6): 453-467.
685 Ashok Jayawant Rao KECHE, G. A. P. R. (2013). "Experimental evaluation of a 35 kVA downdraft
686 gasifier." Front. Energy **7**(3): 300-306.
687 Basu, P. (2006). Combustion and Gasification in Fluidized Beds, CRC Press.
688 Basu, P. (2010). Biomass Gasification and Pyrolysis: Practical Design and Theory, Elsevier Science.
689 Bhattacharjee, S. and A. Dey (2014). "Techno-economic performance evaluation of grid integrated PV-
690 biomass hybrid power generation for rice mill." Sustainable Energy Technologies and
691 Assessments **7**: 6-16.
692 Boiler, A. S. o. M. E. and P. V. Committee (1997). 1995 ASME Boiler & Pressure Vessel Code: An
693 Internationally Recognized Code, American Society of Mechanical Engineers.
694 Coronado, C. R., J. T. Yoshioka, et al. (2011). "Electricity, hot water and cold water production from
695 biomass. Energetic and economical analysis of the compact system of cogeneration run with
696 woodgas from a small downdraft gasifier." Renewable Energy **36**(6): 1861-1868.
697 Daud, A.-K. and M. S. Ismail (2012). "Design of isolated hybrid systems minimizing costs and pollutant
698 emissions." Renewable Energy **44**: 215-224.

699 Elsner, W., M. Wysocki, et al. (2017). "Experimental and economic study of small-scale CHP
700 installation equipped with downdraft gasifier and internal combustion engine." Applied Energy
701 **202**: 213-227.
702 Fanelli, E., A. Viggiano, et al. (2014). "On laminar flame speed correlations for H2/CO combustion in
703 premixed spark ignition engines." Applied Energy **130**: 166-180.
704 Gadsbøll, R. Ø., J. Thomsen, et al. (2017). "Solid oxide fuel cells powered by biomass gasification for
705 high efficiency power generation." Energy **131**: 198-206.
706 Hagos, F. Y., A. R. A. Aziz, et al. (2014). "Trends of Syngas as a Fuel in Internal Combustion Engines."
707 Advances in Mechanical Engineering **6**: 401587.
708 Harish Kumar, R. N. (2013). "Feasibility Study: Photovoltaic Module and Biomass Based Hybrid Power
709 Connected to Grid." South Aust. Context **2**: 14-22.
710 Hazrat, M. A., M. G. Rasul, et al. (2015). "Biofuel: An Australian Perspective in Abating the Fossil Fuel
711 Vulnerability." Procedia Engineering **105**: 628-637.
712 Heywood, J. (1988). Internal Combustion Engine Fundamentals, McGraw-Hill Education.
713 Hsi, C.-L., T.-Y. Wang, et al. (2008). "Characteristics of an Air-Blown Fixed-Bed Downdraft Biomass
714 Gasifier." Energy & Fuels **22**(6): 4196-4205.
715 Hunpinyo, P., P. Cheali, et al. (2014). "Alternative route of process modification for biofuel production
716 by embedding the Fischer–Tropsch plant in existing stand-alone power plant (10MW) based on
717 biomass gasification – Part I: A conceptual modeling and simulation approach (a case study in
718 Thailand)." Energy Conversion and Management **88**: 1179-1192.
719 IEA, I. E. A. (2011). "Energy for all: Financing access for the poor (Chapter 13). World Energy Outlook
720 2011." Retrieved 26 July, 2017, from
721 https://www.iea.org/publications/freepublications/publication/WEO2011_WEB.pdf.

722 IEA, I. E. A. (2016). "Thailand Electricity Security Assessment " Retrieved 26 July, 2017, from
723 https://www.iea.org/publications/freepublications/publication/Partner_Country_Series_Thailand_
724 Electricity_Security_2016_.pdf.
725 Jayah, T. H., L. Aye, et al. (2003). "Computer simulation of a downdraft wood gasifier for tea drying."
726 Biomass and Bioenergy **25**(4): 459-469.
727 Kaaresto, J., I. Ylikoski, et al. (2013). Gasifier, Google Patents.
728 Klein, S. and G. Nellis (2011). Thermodynamics, Cambridge University Press.
729 Kotowicz, J., A. Sobolewski, et al. (2013). "Energetic analysis of a system integrated with biomass
730 gasification." Energy **52**: 265-278.
731 Kumar, P., M. Khare, et al. (2015). "New directions: Air pollution challenges for developing megacities
732 like Delhi." Atmospheric Environment **122**: 657-661.
733 Lapuerta, M., J. J. Hernández, et al. (2001). Thermochemical Behaviour of Producer Gas from
734 Gasification of Lignocellulosic Biomass in SI Engines, SAE International.
735 Lee, S., J. G. Speight, et al. (2014). Handbook of Alternative Fuel Technologies, Second Edition, Taylor
736 & Francis.
737 Lieuwen, T., V. Yang, et al. (2009). Synthesis Gas Combustion: Fundamentals and Applications, CRC
738 Press.
739 Lv, P. M., Z. H. Xiong, et al. (2004). "An experimental study on biomass air–steam gasification in a
740 fluidized bed." Bioresource Technology **95**(1): 95-101.
741 Mainali, B. and S. Silveira (2013). "Alternative pathways for providing access to electricity in
742 developing countries." Renewable Energy **57**: 299-310.
743 Marek, M. (2017). "Numerical simulation of a gas flow in a real geometry of random packed bed of
744 Raschig rings." Chemical Engineering Science **161**: 382-393.

745 Martínez, J. D., K. Mahkamov, et al. (2012). "Syngas production in downdraft biomass gasifiers and its
746 application using internal combustion engines." Renewable Energy **38**(1): 1-9.
747 Materazzi, M., P. Lettieri, et al. (2016). "Performance analysis of RDF gasification in a two stage
748 fluidized bed–plasma process." Waste Management **47**: 256-266.
749 Mayerhofer, M., J. Govaerts, et al. (2011). "Experimental investigation of pressure drop in packed beds
750 of irregular shaped wood particles." Powder Technology **205**(1): 30-35.
751 McKendry, P. (2002). "Energy production from biomass (part 1): overview of biomass." Bioresource
752 Technology **83**(1): 37-46.
753 N., H. K. R. (2014). "Feasibility Study of Photovoltaic (PV) Modules, and Biomass Generator to Supply
754 Electricity to Auckland City, North Island Context-New Zealand." Journal of Clean Energy
755 Technologies **2**(4): 374-378.
756 Network, S. a. D. (2015). "Thais show the way how to power rural areas." Retrieved 26 July, 2017,
757 from http://www.scidev.net/asia-pacific/energy/feature/thais-show-the-way-how-to-power-rural-
758 areas.html.
759 Patuzzi, F., D. Prando, et al. (2016). "Small-scale biomass gasification CHP systems: Comparative
760 performance assessment and monitoring experiences in South Tyrol (Italy)." Energy **112**: 285-
761 293.
762 Pérez, N. P., E. B. Machin, et al. (2015). "Biomass gasification for combined heat and power generation
763 in the Cuban context: Energetic and economic analysis." Applied Thermal Engineering **90**: 1-12.
764 Pode, R., B. Diouf, et al. (2015). "Sustainable rural electrification using rice husk biomass energy: A
765 case study of Cambodia." Renewable and Sustainable Energy Reviews **44**: 530-542.

766 Pradhan, B., Sahoo, Prasad, (2013). "Design of standalone hybrid biomass and PV system of an off-grid
767 house in a remote area." International Journal of Engineering Research and Applications **3**(6):
768 433-437.
769 Pradhan, S. R., P. P. Bhuyan, et al. (2013). Design of standalone hybrid biomass and PV system of an
770 off-grid house in a remote area.
771 Products, A. P. L.-C. N. P. (2012). "Biomass to Woodgas to BTU to HP to KW to MPG conversion
772 rules." Retrieved 26 July, 2017, from
773 http://wiki.gekgasifier.com/w/page/6123680/Biomass%20to%20Woodgas%20to%20BTU%20to
774 %20HP%20to%20KW%20to%20MPG%20conversion%20rules.
775 Przybyla, G., A. Szlek, et al. (2016). "Fuelling of spark ignition and homogenous charge compression
776 ignition engines with low calorific value producer gas." Energy **116**: 1464-1478.
777 Rajbongshi, R., D. Borgohain, et al. (2017). "Optimization of PV-biomass-diesel and grid base hybrid
778 energy systems for rural electrification by using HOMER." Energy **126**: 461-474.
779 Rao, K. R. (2009). Companion Guide to the ASME Boiler & Pressure Vessel Code: Criteria and
780 Commentary on Select Aspects of the Boiler & Pressure Vessel and Piping Codes, ASME Press.
781 Reed, T., T. B. R. A. Das, et al. (1988). Handbook of Biomass Downdraft Gasifier Engine Systems,
782 Biomass Energy Foundation.
783 Röder, M., C. Whittaker, et al. (2015). "How certain are greenhouse gas reductions from bioenergy? Life
784 cycle assessment and uncertainty analysis of wood pellet-to-electricity supply chains from forest
785 residues." Biomass and Bioenergy **79**: 50-63.
786 Salas, V., W. Suponthana, et al. (2015). "Overview of the off-grid photovoltaic diesel batteries systems
787 with AC loads." Applied Energy **157**: 195-216.

788 Samiran, N. A., M. N. M. Jaafar, et al. (2016). "Progress in biomass gasification technique – With focus
789 on Malaysian palm biomass for syngas production." Renewable and Sustainable Energy Reviews
790 **62**: 1047-1062.
791 Sattar, A., G. A. Leeke, et al. (2014). "Steam gasification of rapeseed, wood, sewage sludge and
792 miscanthus biochars for the production of a hydrogen-rich syngas." Biomass and Bioenergy **69**:
793 276-286.
794 Singh, A. and P. Baredar (2016). "Techno-economic assessment of a solar PV, fuel cell, and biomass
795 gasifier hybrid energy system." Energy Reports **2**: 254-260.
796 Singh, S., M. Singh, et al. (2016). "Feasibility study of an islanded microgrid in rural area consisting of
797 PV, wind, biomass and battery energy storage system." Energy Conversion and Management
798 **128**: 178-190.
799 Sukamongkol, Y., S. Chungpaibulpatana, et al. (2002). "A simulation model for predicting the
800 performance of a solar photovoltaic system with alternating current loads." Renewable Energy
801 **27**(2): 237-258.
802 Thomsen, T. P., Z. Sárossy, et al. (2017). "Low temperature circulating fluidized bed gasification and
803 co-gasification of municipal sewage sludge. Part 1: Process performance and gas product
804 characterization." Waste Management **66**: 123-133.
805 Warren, T. J. B., R. Poulter, et al. (1995). "Converting biomass to electricity on a farm-sized scale using
806 downdraft gasification and a spark-ignition engine." Bioresource Technology **52**(1): 95-98.
807 Yamegueu, D., Y. Azoumah, et al. (2011). "Experimental study of electricity generation by Solar
808 PV/diesel hybrid systems without battery storage for off-grid areas." Renewable Energy **36**(6):
809 1780-1787.

Zainal, Z. A., A. Rifau, et al. (2002). "Experimental investigation of a downdraft biomass gasifier." Biomass and Bioenergy **23**(4): 283-289.

Highlights

- A hybrid syngas/solar PV/battery system is proposed at a prototype scale study.
- Syngas genset plays a key role on complementing the intermittence of solar energy.
- The preliminary commissioning shows promising potential in continuous supplying.
- Working efficiency of solar PV system at shortage energy are important variable.
- Optimization and effective scale-up of the proposed system will further be studied.

Manuscript submission for consideration for possible publication in Chemical Engineering Research and Design (SI: Energy System Engineering)

832

833

834

835

Design and preliminary operation of a hybrid syngas/solar PV /battery power system for off-grid applications: A case study in Thailand

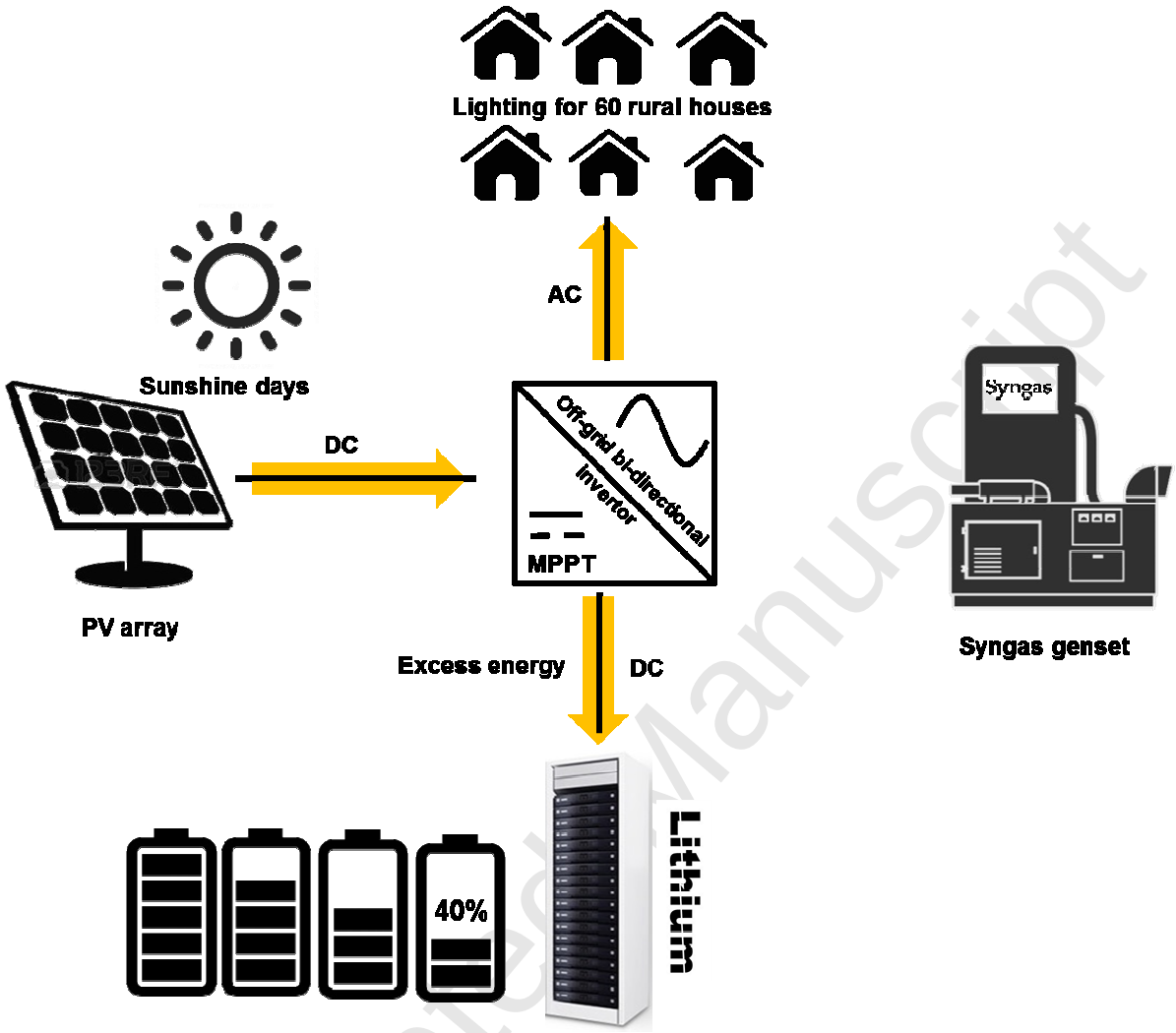

(a)

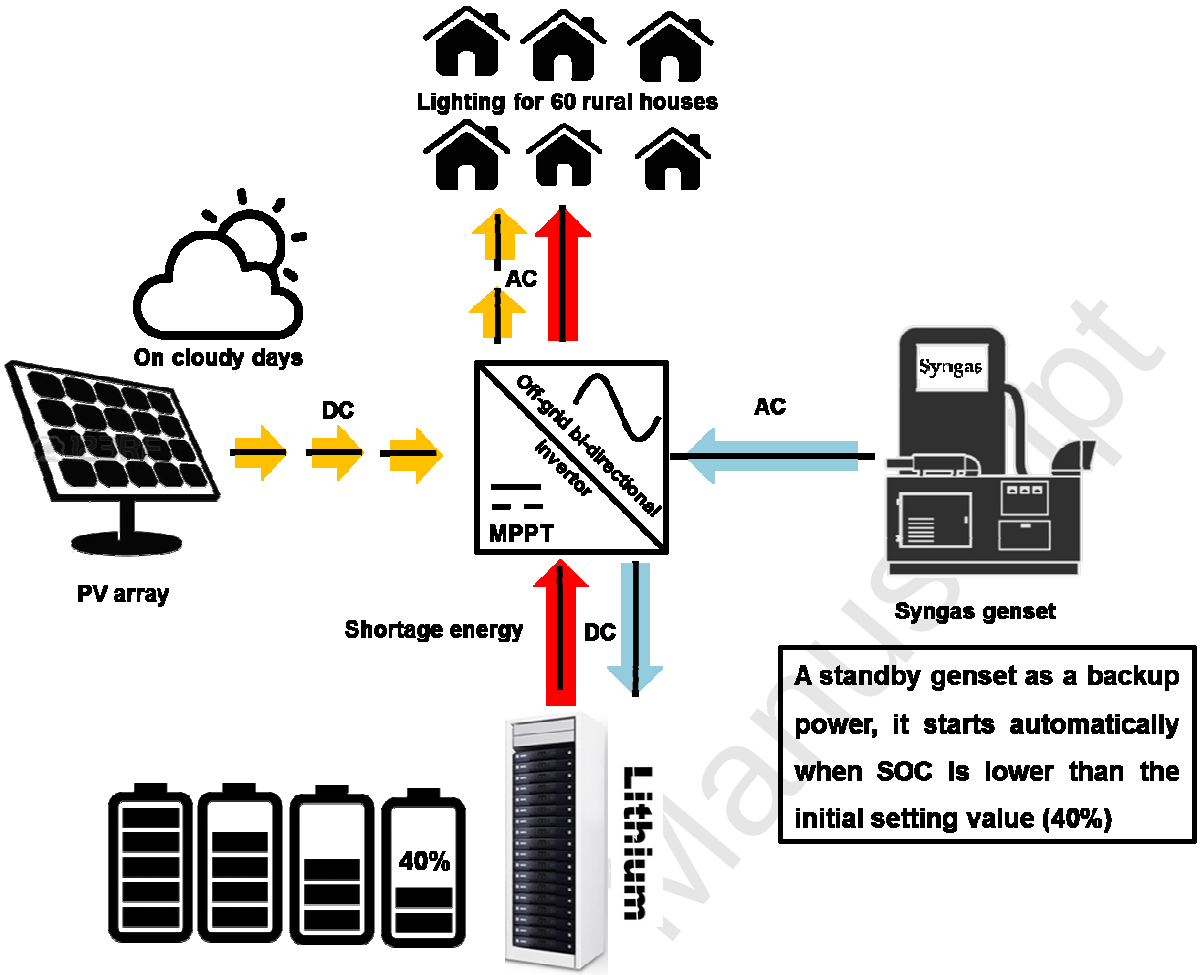

(b)

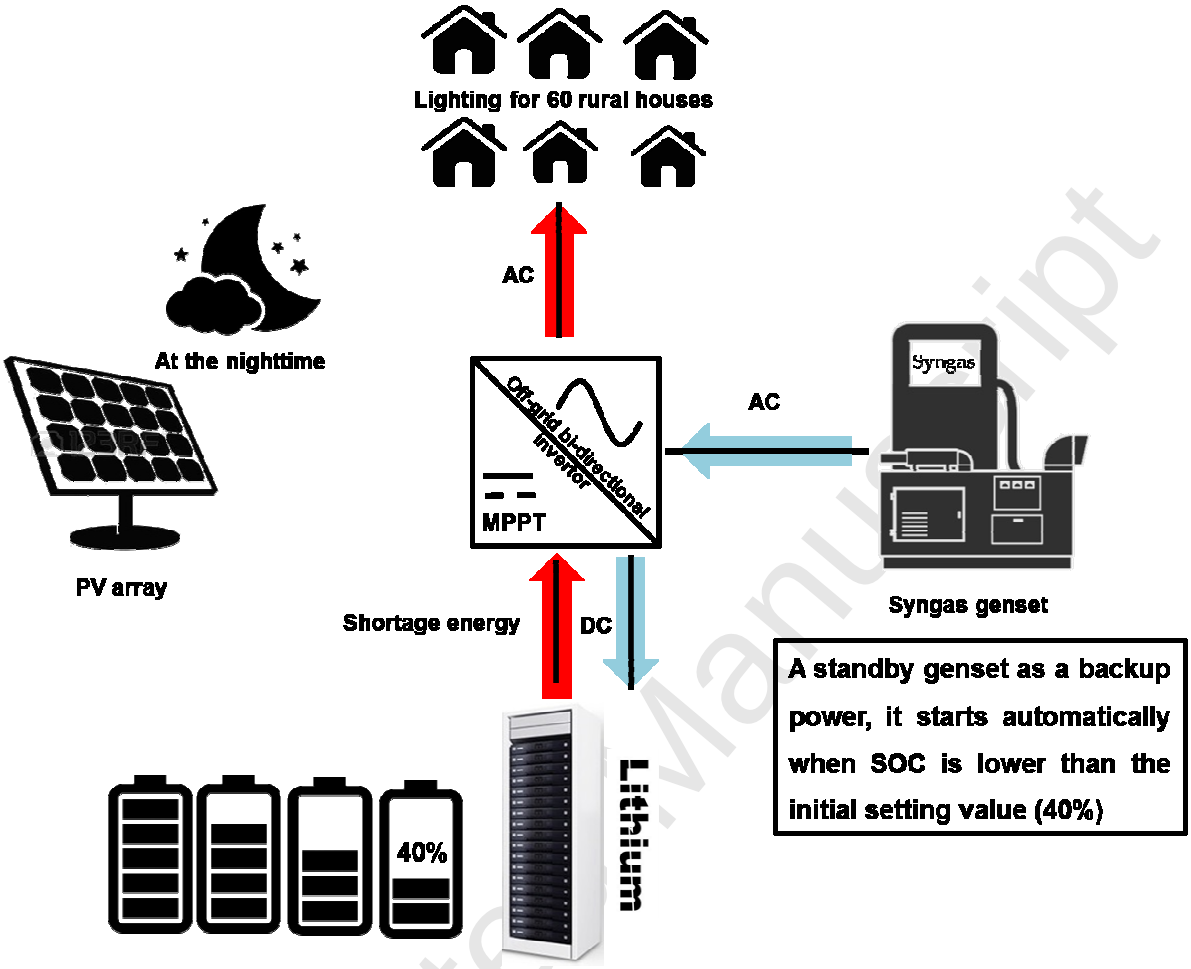

(c)

Fig. 1 Dispatch strategy of hybrid syngas/solar/battery system through off-grid bi-directional inverter: on two scenarios (a) the excess energy, (b) and (c) the shortage energy.

Fig. 2 Torrefied rubber wood pellet used for gasification. Pellets are 10 mm diameter cylinders of average 50–150 mm length.

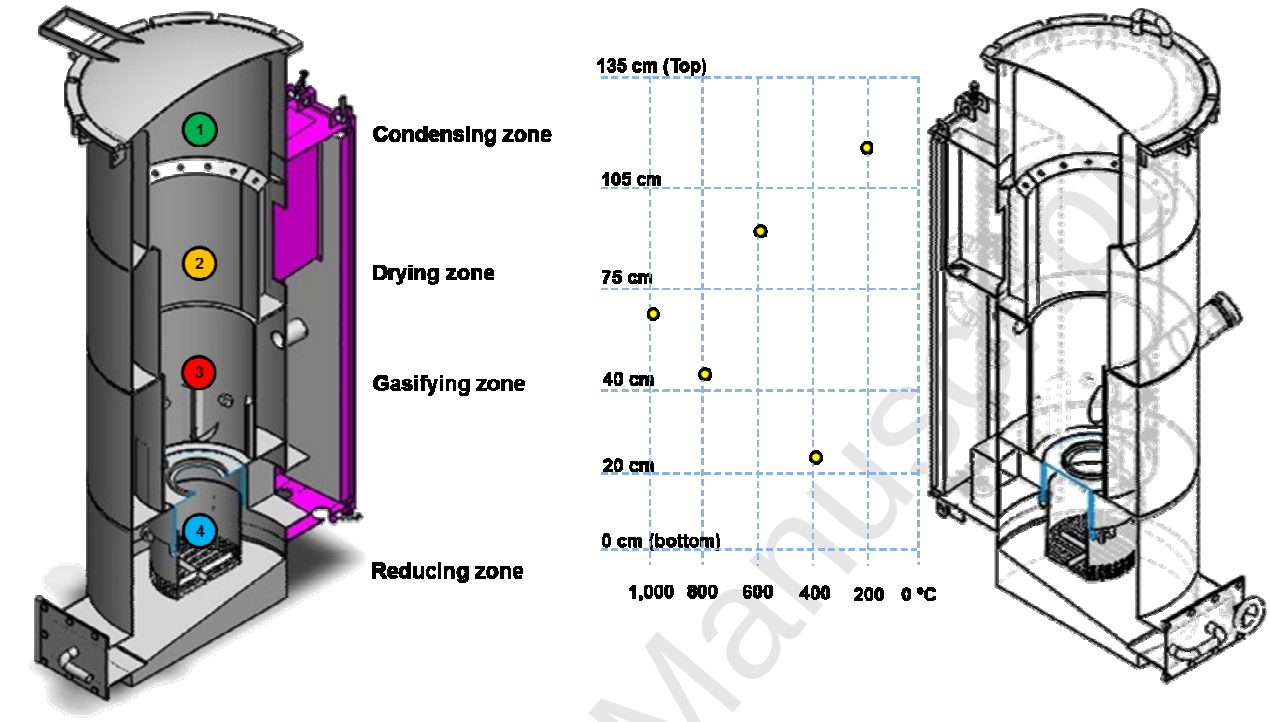

Fig. 3 Schematic diagram of modified downdraft reactor (approximately 40-50 kg/h) and its typical temperature profile through gasifier during operation

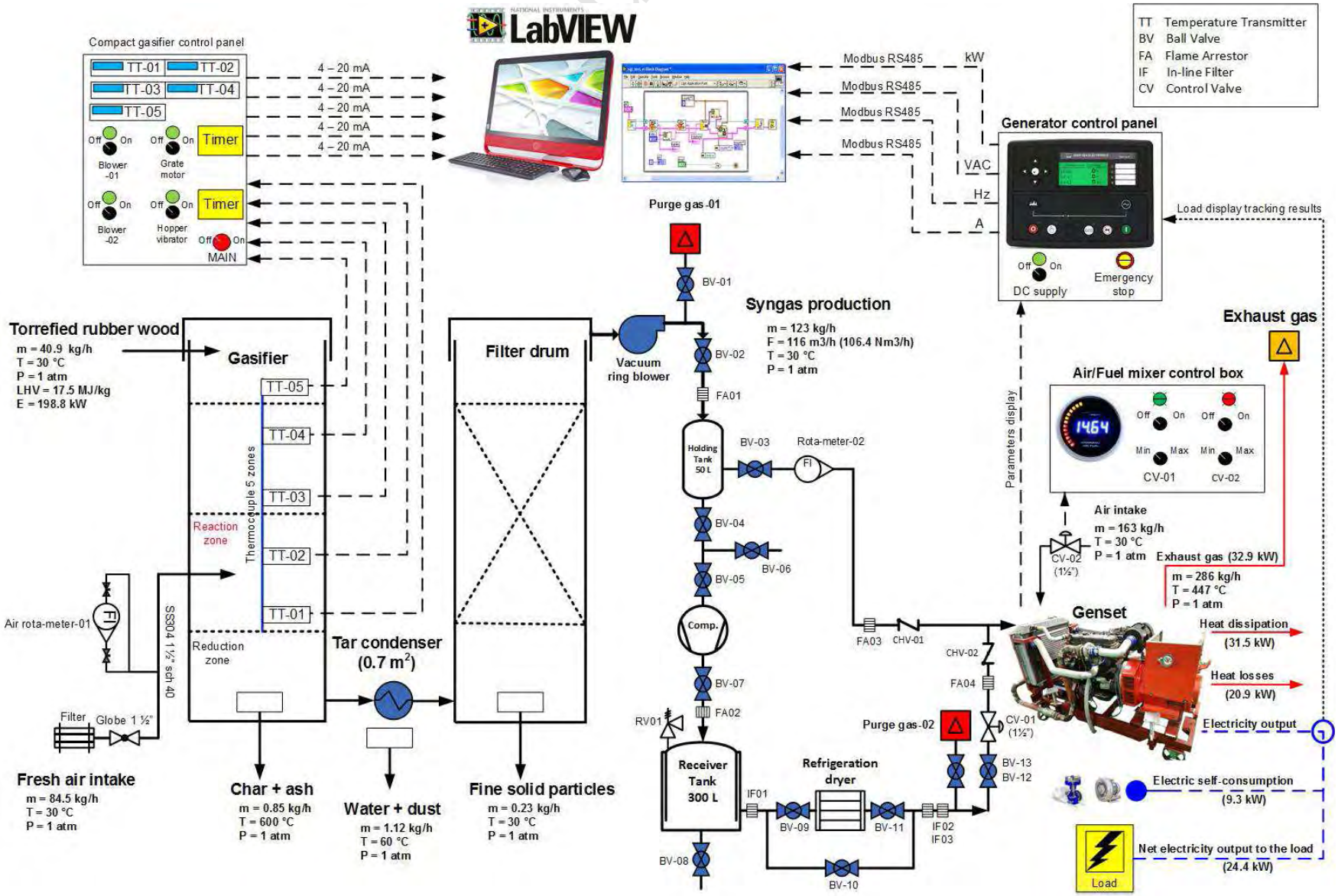
LabVIEW
Compact gasifier control panel
TT-01
TT-02
TT-03
TT-04
TT-05
Timer
Blower -01
Grate motor
Blower -02
Hopper vibrator
MAIN
4 – 20 mA
Modbus RS485
kW
VAC
Hz
A
TT Temperature Transmitter
BV Ball Valve
FA Flame Arrestor
IF In-line Filter
CV Control Valve
Generator control panel
DC supply
Emergency stop
Load display tracking results
Purge gas-01
BV-01
Syngas production
m = 123 kg/h
F = 116 m3/h (106.4 Nm3/h)
T = 30 °C
P = 1 atm
Torrefied rubber wood
m = 40.9 kg/h
T = 30 °C
P = 1 atm
LHV = 17.5 MJ/kg
E = 198.8 kW
Gasifier
Reaction zone
Reduction zone
Thermocouple 5 zones
Filter drum
Vacuum ring blower
BV-02
FA01
Holding Tank 50 L
BV-03
Rota-meter-02
BV-04
BV-06
BV-05
Comp.
BV-07
FA02
RV01
Receiver Tank 300 L
BV-08
Refrigeration dryer
IF01
BV-09
BV-11
IF02
IF03
BV-10
Air rota-meter-01
SS304 1½" sch 40
Filter
Globe 1 ½"
Fresh air intake
m = 84.5 kg/h
T = 30 °C
P = 1 atm
Char + ash
m = 0.85 kg/h
T = 600 °C
P = 1 atm
Tar condenser (0.7 m²)
Water + dust
m = 1.12 kg/h
T = 60 °C
P = 1 atm
Fine solid particles
m = 0.23 kg/h
T = 30 °C
P = 1 atm
Exhaust gas
Air/Fuel mixer control box
1464
CV-01
CV-02
Parameters display
Air intake
m = 163 kg/h
T = 30 °C
P = 1 atm
CV-02 (1½")
Exhaust gas (32.9 kW)
m = 286 kg/h
T = 447 °C
P = 1 atm
Genset
FA03
CHV-01
CHV-02
FA04
Purge gas-02
CV-01 (1½")
BV-13
BV-12
Heat dissipation (31.5 kW)
Heat losses (20.9 kW)
Electricity output
Electric self-consumption (9.3 kW)
Load
Net electricity output to the load (24.4 kW)

Fig. 4 Process and Instrument Diagram (P&ID) layout of the proposed biomass-fueled genset system connecting with the mass and energy balances

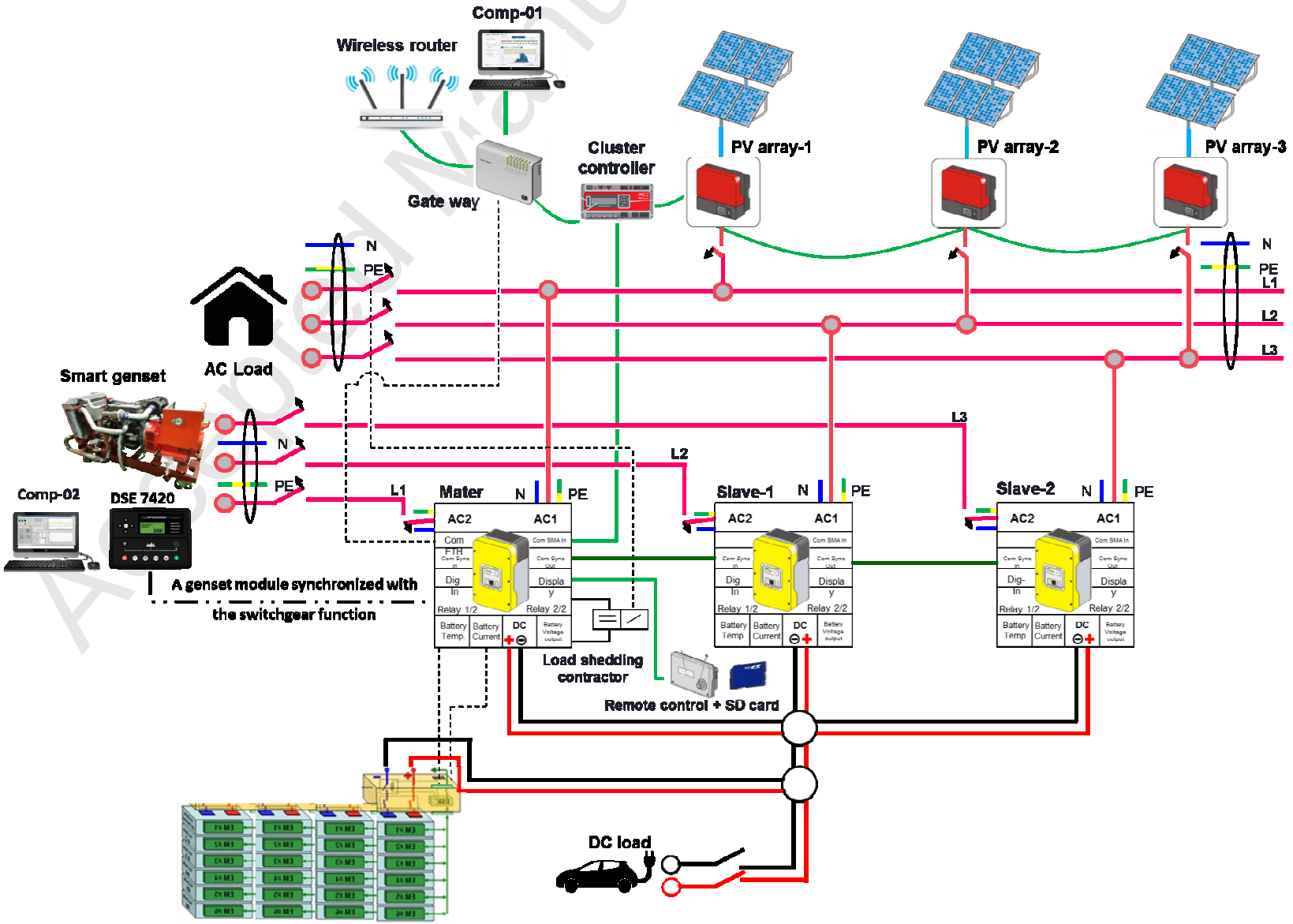

Fig. 5 Proposed electrical diagram of a hybrid syngas/solar PV /battery power system for off-grid applications

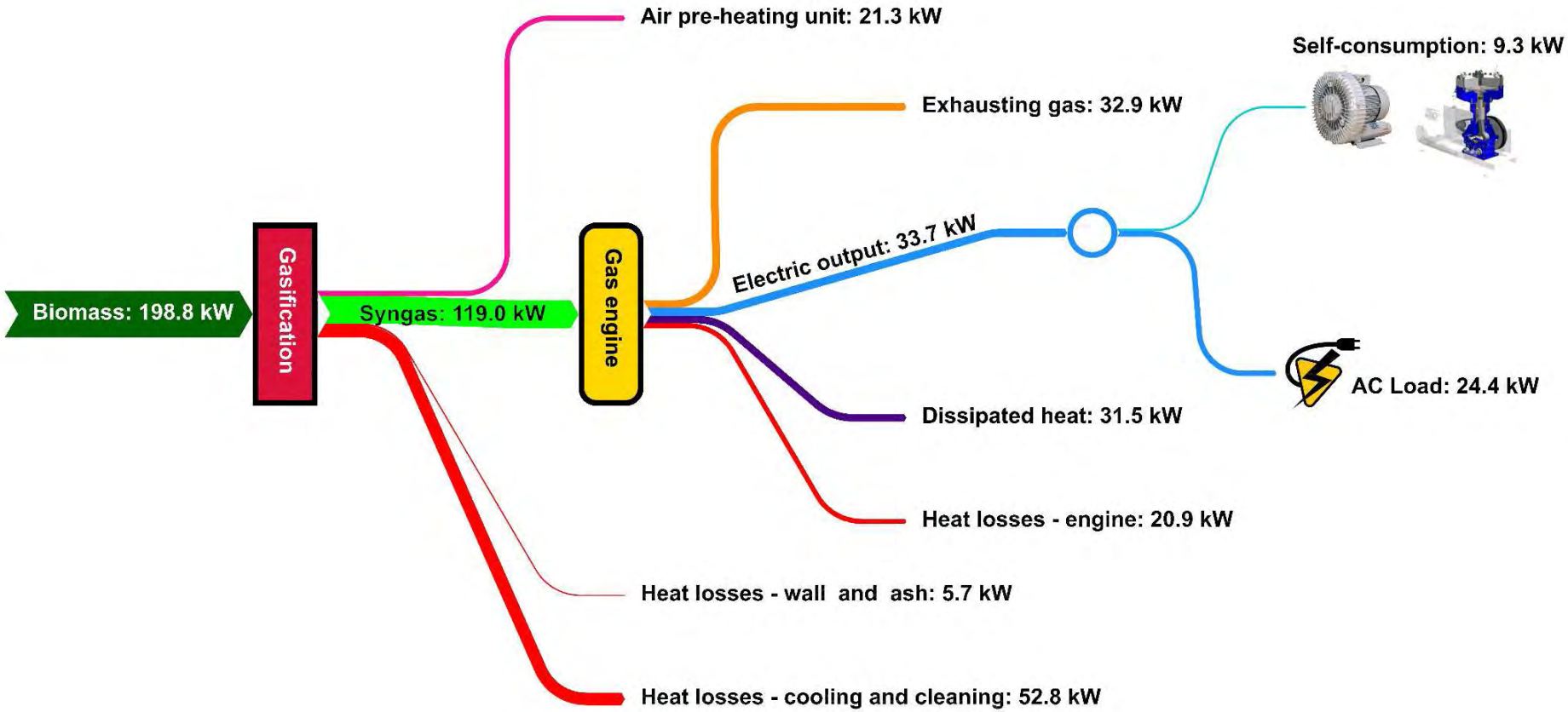

Fig. 6 A Sankey diagram of energy flows for the integrated biomass gasification and engine/generator systems

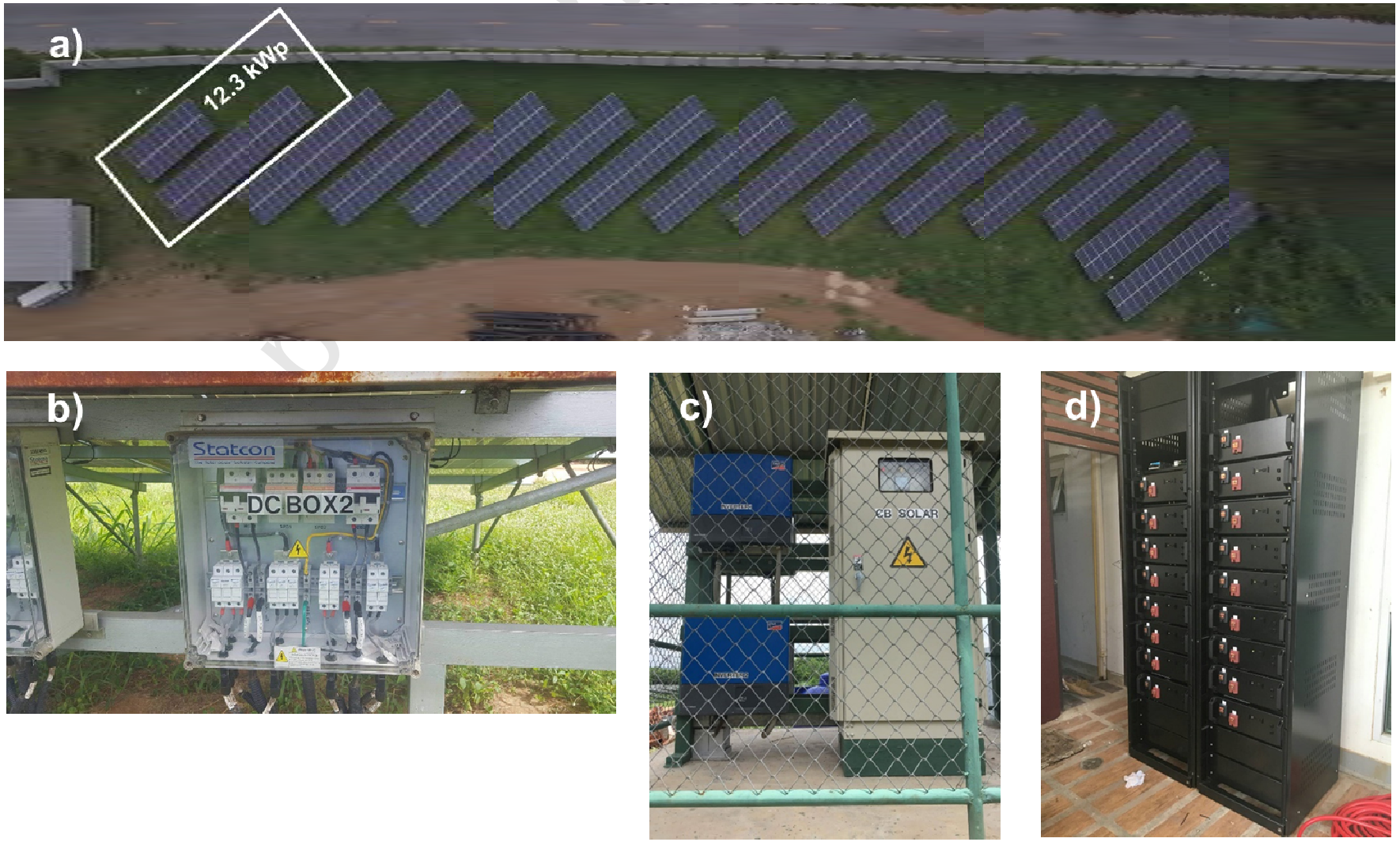
a)
12.3 kWp
b)
Statcon
DC BOX2
c)
CB SOLAR
d)

Fig. 7 The top view photo taken with a drone on the map located 12° 49' 40.6" N latitude and 101° 13' 06.1"E longitude (KMUTNB Rayong Campus) - a) 12.3 kWp of solar power separated to study for the proposed hybrid system, b) Circuit breakers, c) PV inverters and d) Batteries storage

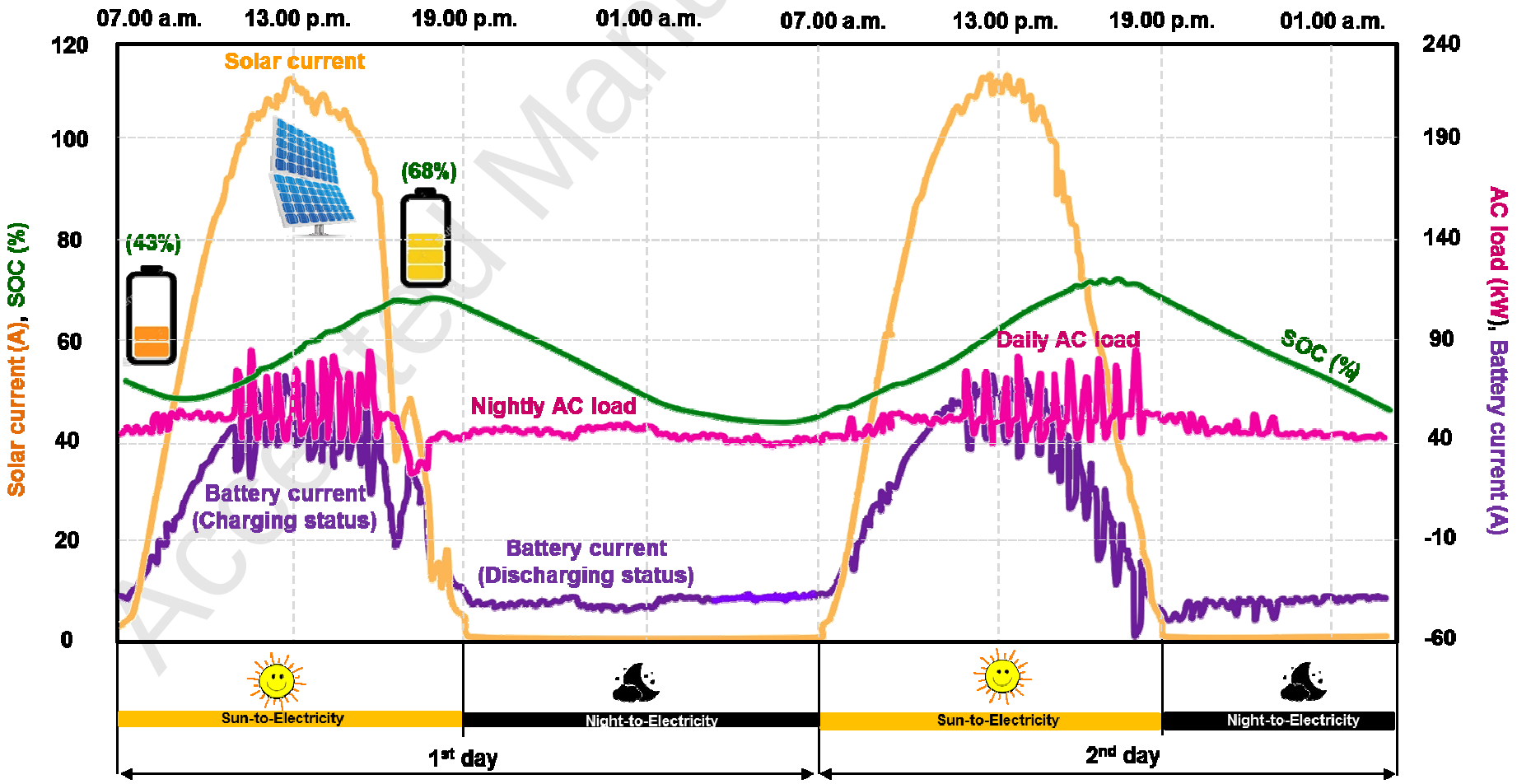

Fig. 8 Power profiles of a hybrid solar PV/battery system without a standby syngas genset

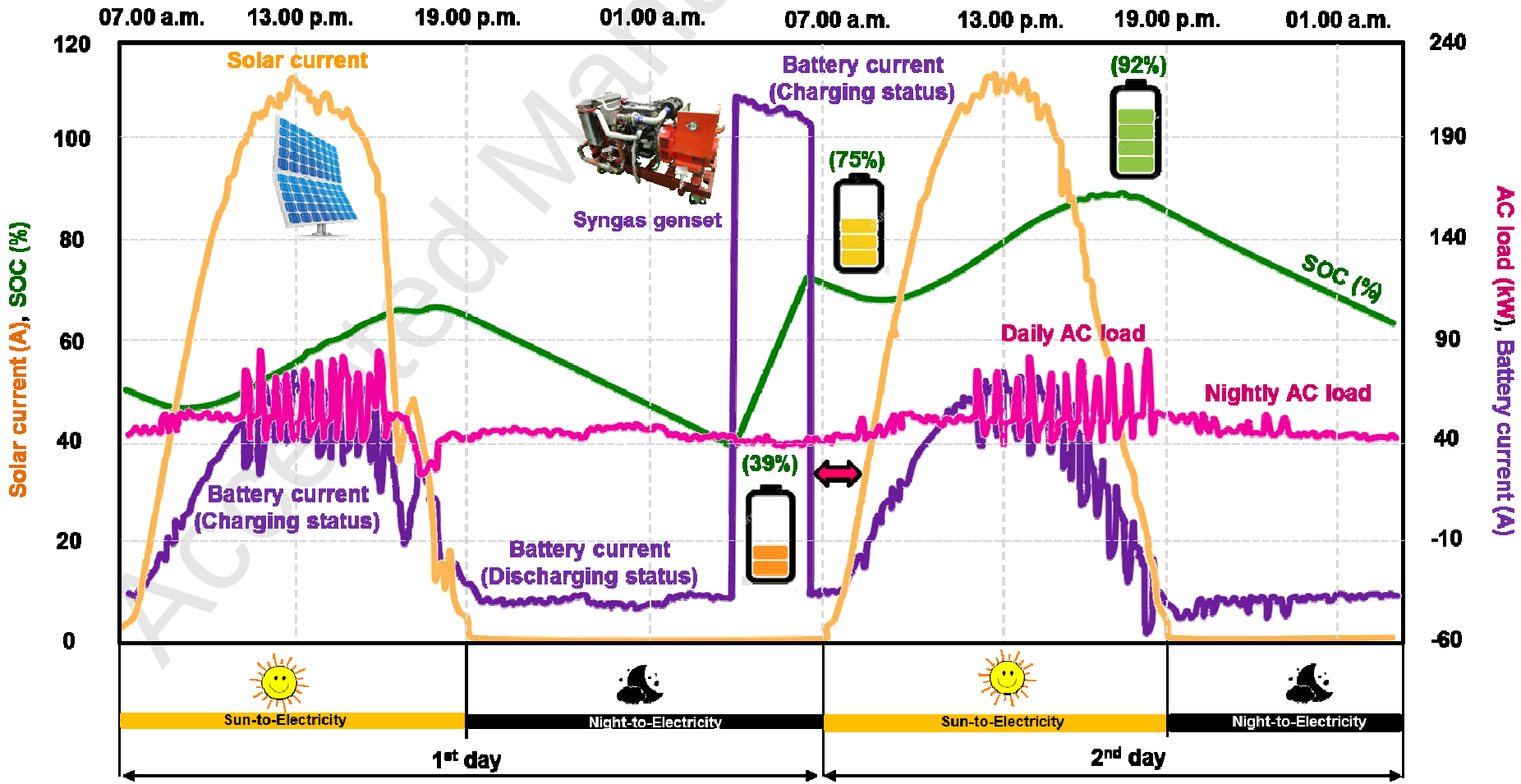

Fig. 9 Power profiles of a hybrid solar PV/battery system with a standby syngas genset

Table 1 Chemical characterization of local torrefied rubber wood tested in gasifier.

Characterization	Proposed this study
Moisture content (wt. %) (ASTM D 3302)	7.82
Proximate analysis (wt.% dry)	Torrefied rubber wood
• Ash (ASTM D 73174)	1.9
• Volatile matter (ASTM D 3175)	81.8
• Fixed carbon (ASTM D 3172)	16.3
Ultimate analysis (wt. % dry)	
• C	49.1
• H	6.0
• N	-
• S (ASTM D 5865)	-
• O	43.0
• Cl	-
• Ash (ASTM D 73174)	1.9
• $HHV_{d.b}$ (MJ/kg) (ASTM D 5865)	19.0
• $LHV_{d.b}$ (MJ/kg) (ASTM D 5865)	17.5
Bulk density (kg/m^3)	576

Table 2 Overall performances of a modified genset fuelled with torrefied rubber wood syngas

Engine main data before modification	Description
- Engine model	Isuzu Diesel 4BC2 (Made in Japan)
- Year production	1982-1987
- Type car	Isuzu ELF and NPR trucks
- Horse power	65 kw (105 hp) at 3500 rpm
- Torque	200 N·m at 2200 rpm
- Bore diameter	102 mm
- Stroke	80 mm
- Displacement (D)	3.3 Liter
- Number of Cylinder	4 cylinders
- Injection system	Direct injection
Setting configuration parameters for syngas engine	Description
- Modified in the diesel engine	Ignition system
- Air metering	VGT, intercooler
- Revolution per minute (RPM)	1500
- Compression ratio (CR)	11.5:1
- Syngas fuelled (%)	100
- Spark timing (º BTDC)	28
- Power de-rating[a] (%)	20[b]
- Combustion A/F ratio	1.32[c]
Setting configuration parameters for generator	Description
- Alternator	STAMFORD
- Maximum continuous capacity	45 kVA
- Phase	3 Phase - P.F 0.8
- Speed	1500 rpm - 4 Pole
- Frequency	50 Hz
- Construction	Single bearing

a Calculated as a fraction of a nominal engine power.
b Assuming the alternator and transmission efficiency of 80% and 95% respectively.
c Air/Fuel (syngas) mass ratio = 163 kg/h / 123 kg/h = 1.32.

Table 3 The balance of mass streams on the combined thermal and power system (a) biomass air gasification and (b) engine/generator

(a) Descriptive parameters of biomass air gasification unit

Run	Equivalent ratio (φ)[a]	Air flowrate (Nm^3/h)	Total input (kg/h)		Total output (kg/h)					Mass balance closure (%) [b]
			Air flowrate (kg/h) @ 1.76 wt% moist.	Wood consumption rate (kg/h) @ 7.82 wt% moist.	Syngas flow rate (kg/h)	Syngas flow rate (Nm^3/h)	Char + ash at gasifier	Wood vinegar + dust at condenser	Fine solid particles at filter tank	
1	0.34	72.5	84.5	40.9	123	106.4	0.85	1.12	0.23	99.8

[a] A detail of calculation is listed in Supplementary Data Appendix A (see more in Equation (1))
[b] A detail of mass balance closure is calculated to be (125.2/125.4) x 100 = 99.8% (please find the information requested in Table 3b)

(b) Mass balance of biomass air gasification unit

Input material streams	kg/h
1. Torrefied biomass pellets	40.9
2. Fresh air intake	84.5
Total (1) + (2)	**125.4**

Output material streams	kg/h
I. Char + ash	0.85
II. Wood vinegar + dust	1.12
III. Fine solid particles	0.23
IV. Syngas production	123
Total (I) +… (IV)	**125.2**

(c) Mass balance of engine/generator unit

Input material streams	kg/h
1. Syngas	123
2. Fresh air intake	163
Total (1) + (2)	**286**

Output material streams	kg/h
I. Exhaust gas	286
Total (I) +… (IV)	**286**

Design and preliminary operation of a hybrid syngas/solar PV /battery power system for off-grid applications: A case study in Thailand

Table 4 Main gasifier performance parameters[a]

Description	Unit	Value
Carbon conversion efficiency[a]	(%), η_{CCE}	90.88
Cold gas efficiency[a]	(%), η_{CGE}	59.85
Dry syngas yield[a]	(Nm^3/kg), Y_{gas}	2.82
Dry syngas low heating value[a]	(MJ/Nm^3)	4.027
Syngas flowrate	(Nm^3/h)	106.43
Produced syngas content (volumetric)	H_2 (%)	13.5
	CO (%)	16.5
	CO_2 (%)	12.0
	CH_4 (%)	1.4
	N_2 (%)	55.7
Tar	mg/Nm^3	48.5
Char and ashes	kg/Nm^3	0.008

[a] Details of calculation are listed in Supplementary Data Appendix A (see more in Equation (2) to (5))

Table 5 Electricity, thermal and overall efficiencies for the proposed system

Characteristics of output parameters	**Experimental results**	**Units**
- Exhaust gas temperature	447	(ºC)
- Net Electric power output	33.7	(kW)
- Useful heat output	32.9	(kW)
Characteristics of output efficiencies	**Experimental results**	**Units**
- Overall process efficiency ($\eta_{overall}$) [a]	44.21	%
- Gas engine efficiency (η_{engine}) [b]	28.32	%
- Electrical efficiency ($\eta_{electricity}$) [c]	16.95	%
- Power station efficiency (η_{power}) [d]	12.27	%
- Thermal efficiency ($\eta_{thermal}$) [e]	27.26	%

a Usable heat and net electric power output are produced from engine/generator system (see more in Equation (6) of Supplementary Data Appendix A)
b Syngas is produced from gasification process (see more in Equation (7) of Supplementary Data Appendix A)
c Net electric power output is produced from engine/generator system (see more in Equation (8) of Supplementary Data Appendix A)
d Electric power output is supplied to the load (see more in Equation (9) of Supplementary Data Appendix A)
e Net usable heat is produced from engine/generator system (see more in Equation (10) of Supplementary Data Appendix A)

Table 6 Energy balance for the proportion of losses and thermal outputs and electrical production

Proportion of Electricity production	**Value**	**Unit**	**Percentage**
(1) Electrical self-consumption (auxiliary as blower, compressor etc.)	9.3	kWe	4.7%
(2) Electrical supply to the load	24.4	kWe	12.3%
• Net electricity generation (1) + (2)	33.7	kWe	17%
Proportion of thermal production	**Value**	**Unit**	**Percentage**
(3) Exhausting gas for useful the biomass drying process	32.9	kWth	16.5%
(4) Dissipated heat as turbocharger, intercooler etc.	31.5	kWth	15.8%
(5) Air pre-heating unit	21.3	kWth	10.7%
• Net thermal output (3) + (4) + (5)	85.7	kWth	43%
Loss fractions	**Value**	**Unit**	**Percentage**
(6) Heat losses - wall and ash	5.7	kWth	2.9%
(7) Heat losses - cooling and purification	52.8	kWth	26.6%
(8) Heat losses - engine	20.9	kWth	10.5%
• Total losses in the whole process (6) + (7) + (8)	79.4	kWth	40%
Total (1) + (2) + … + (7) + (8)	**198.8**	**kWth**	**100%**

Design and preliminary operation of a hybrid syngas/solar PV /battery power system for off-grid applications: A case study in Thailand

Graphical abstract

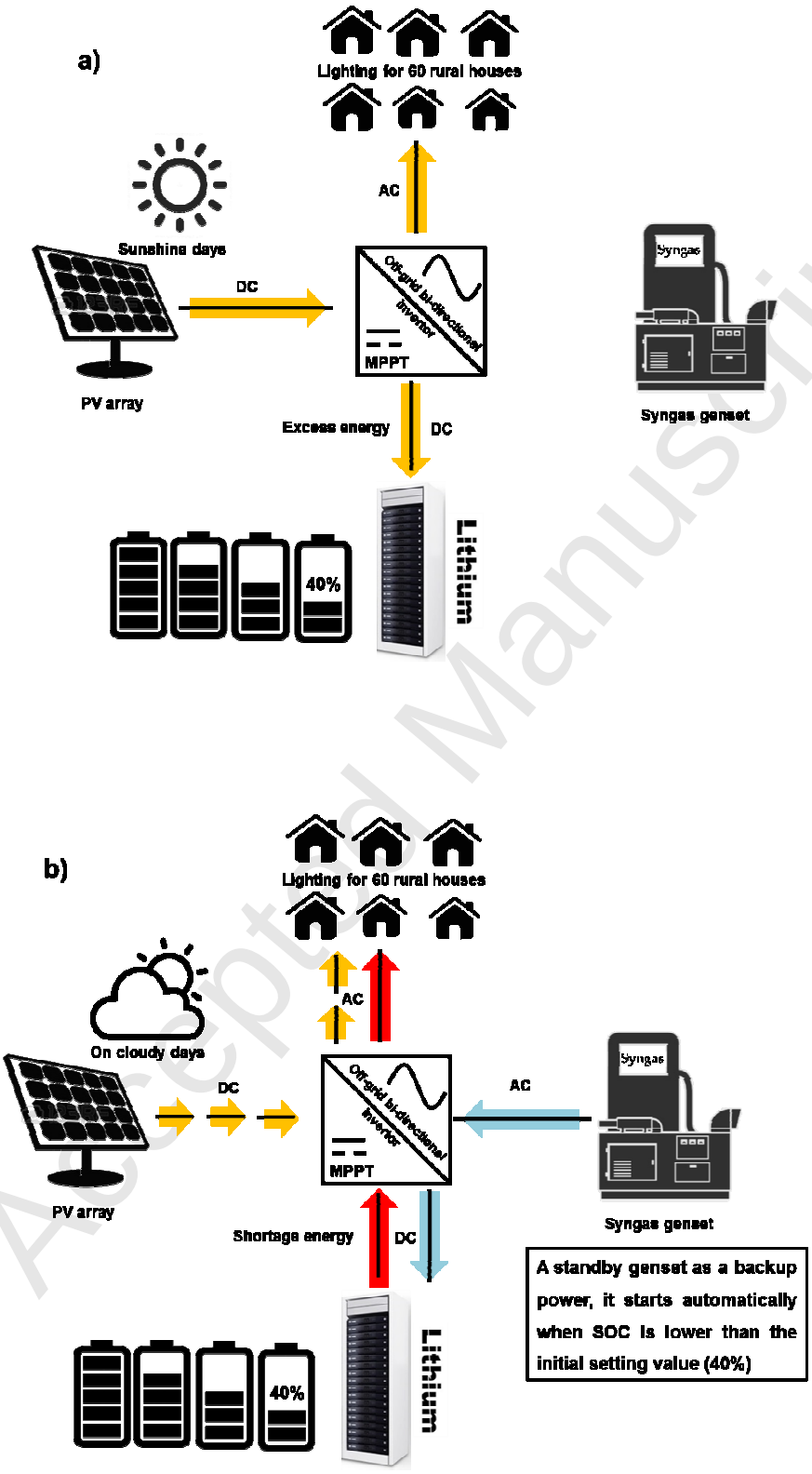

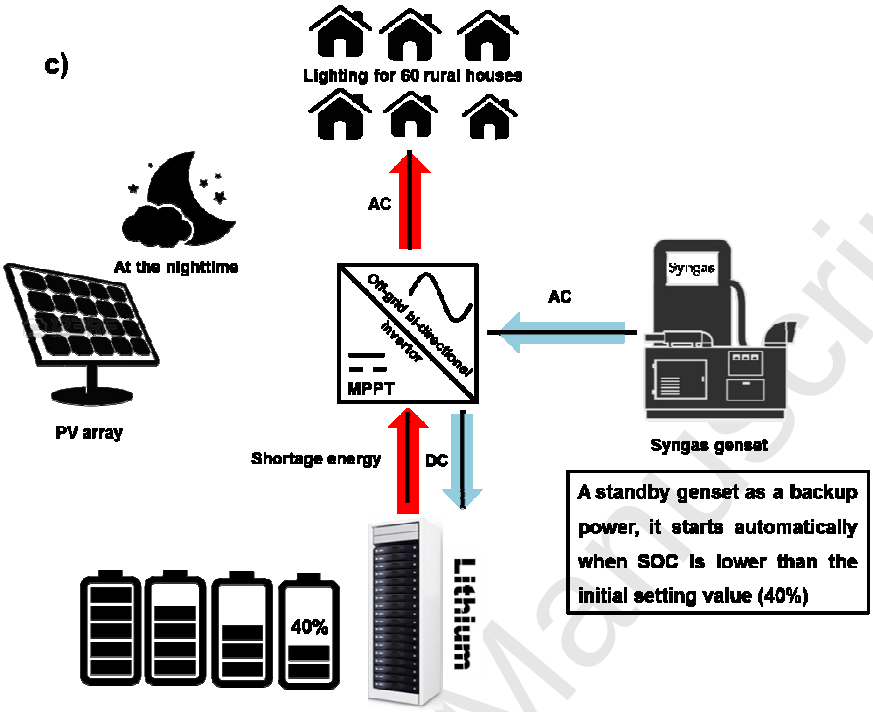

Due to the discontinuous nature of solar energy, a hybrid power system could be designed by incorporating biomass gasification and electricity generation to PV array and battery storage system. It can be used as backup power generation to improve the stability and reliability of system when occurred in case of shortage of energy e.g. (b) on cloudy day and (c) at the nighttime.